

**CINTAL - Centro de Investigação Tecnológica do Algarve**  
**Universidade do Algarve**

## **Calibration of Dual Accelerometer Vector Sensor**

N. Pinto and S.M. Jesus

Rep 04/20 - SiPLAB

September 23, 2020

University of Algarve  
Campus de Gambelas  
8005-139, Faro,  
Portugal

tel: +351-289244422  
fax: +351-289864258  
cintal@ualg.pt  
www.cintal.ualg.pt

Work requested by	CINTAL Universidade do Algarve, Campus de Gambelas 8005-139 Faro, Portugal Tel: +351-289244422, cintal@ualg.pt, www.cintal.ualg.pt
Laboratory performing the work	SiPLAB - Signal Processing Laboratory Universidade do Algarve, FCT, Campus de Gambelas, 8005-139 Faro, Portugal tel: +351-289800949, info@siplab.fct.ualg.pt, www.siplab.fct.ualg.pt
Project	EMSO-PT
Title	DAVS calibration report
Authors	N. Pinto and S.M. Jesus
Date	September 23, 2020
Reference	04/20 - SiPLAB
Number of pages	59 (fifty nine)
Abstract	This report discusses the acoustic calibration of the Dual Accelerometer Vector Sensor (DAVS) carried out at the Arsenal do Alfeite acoustic tank, in Lisbon, on 17 <sup>th</sup> and 18 <sup>th</sup> of November 2016. This is a revision of previous report SiPLAB 4/17 of April 2017 [1], with a more comprehensive description of the tank limitations as well as the signal path and processing steps for obtaining calibrated curves for sensitivity and directivity in the band 0.5 to 4kHz. Additional results from previously unprocessed data, not included in the previous report, are given for accelerometers data captured when device Z axis is pointing to the source.
Clearance level	UNCLASSIFIED
Distribution list	SiPLAB(1), CINTAL(1)
Total number of copies	2 (two)

Copyright Cintal@2020

**Approved for publication**

A.B. Ruano

President Administration Board

# Contents

<b>Cover</b>	<b>1</b>
<b>Abstract</b>	<b>1</b>
<b>1 Introduction</b>	<b>2</b>
<b>2 DAVS calibration test at the Arsenal tank</b>	<b>3</b>
2.1 Theoretic propagation times for the Arsenal tank . . . . .	3
2.2 DAVS sensitivity test . . . . .	4
2.3 DAVS directivity test . . . . .	6
<b>3 DAVS signal path</b>	<b>8</b>
3.1 DAVS hydrophone forward and backward signal path . . . . .	8
3.1.1 Voltage at hydrophone terminals . . . . .	9
3.1.2 DAVS hydrophone pre-amplifier gain . . . . .	9
3.1.3 DAVS hydrophone programmable gain amplifier (PGA) . . . . .	10
3.1.4 DAVS hydrophone single ended to differential . . . . .	10
3.1.5 DAVS hydrophone ADC / WAVE file . . . . .	10
3.1.6 DAVS hydrophone full forward and backward path . . . . .	11
3.2 DAVS accelerometer forward and backward signal path . . . . .	11
3.2.1 Accelerometer sensitivity . . . . .	11
3.2.2 DAVS accelerometer PGA, single ended to differential and AD- C/WAVE file . . . . .	12
3.2.3 DAVS Accelerometer full forward and backward path . . . . .	12
<b>4 DAVS Calibration - Data Processing</b>	<b>14</b>
4.1 DAVS sensitivity analysis methodology . . . . .	14
4.2 DAVS sensitivity analysis . . . . .	15
4.3 DAVS directivity analysis methodology . . . . .	17
4.4 DAVS directivity analysis . . . . .	18
4.4.1 Directivity diagram at 2 kHz . . . . .	18
4.4.2 Directivity diagram at 3 kHz . . . . .	19
4.4.3 Directivity diagram at 4 kHz . . . . .	19
<b>5 Results and Conclusions</b>	<b>22</b>
<b>Bibliography</b>	<b>24</b>
<b>Appendices</b>	<b>25</b>
A DAVS additional formulas . . . . .	25
A.1 Hydrophone Sensitivity . . . . .	25
B DAVS Sensitivity Waveforms . . . . .	26
B.1 Y Axis Sensitivity at 1 kHz . . . . .	26
B.2 Y Axis Sensitivity at 2 kHz . . . . .	28

B.3	Y Axis Sensitivity at 3 kHz . . . . .	29
B.4	Y Axis Sensitivity at 4 kHz . . . . .	31
B.5	Z Axis Sensitivity at 0.5 kHz . . . . .	32
B.6	Z Axis Sensitivity at 1 kHz . . . . .	34
B.7	Z Axis Sensitivity at 2 kHz . . . . .	35
B.8	Z Axis Sensitivity at 3 kHz . . . . .	37
B.9	Z Axis Sensitivity at 4 kHz . . . . .	38
B.10	Y Axis Accelerometer voltage waveforms . . . . .	40
B.11	3 Axis Accelerometers voltage waveforms for Y axis experiment . .	41
B.12	Z Axis Accelerometer voltage waveforms . . . . .	42
B.13	3 Axis Accelerometers voltage waveforms for Z axis experiment . .	43
C	DAVS Directivity Waveforms . . . . .	44
C.1	Directivity Comparison . . . . .	44
C.2	Setup 1 at 2 kHz . . . . .	45
C.3	Setup 1 at 3 kHz . . . . .	47
C.4	Setup 1 at 4 kHz . . . . .	49
C.5	Setup 2 and 3 at 2 kHz . . . . .	51

# List of Figures

2.1	Theoretical propagation times for the Arsenal tank, with transducers at mid depth and various source - receiver distances (X axis). Note that the top and bottom reflected times are overlapped. . . . .	4
2.2	Sensitivity experiment setup for Z axis test. . . . .	6
2.3	Setup placement for Y axis sensitivity experiment. . . . .	6
2.4	Three setups and placement of devices used for directivity measurements. Note that the clockwise and then the counter clockwise rotation were used for the experiments. . . . .	7
3.1	DAVS hydrophone signal path: from sensor (left) to digital WAVE file (right). . . . .	9
3.2	Accelerometer signal path: the accelerometer (left) to the digital WAVE file (right). . . . .	12
4.1	Obtained hydrophone (left graph) and accelerometer sensitivities (right graph), for the 2 used orientations (Y and Z pointing to source) . . . .	16
4.2	Comparison of sensor sensitivities (Y axis pointing to source) between values obtained in the report [1] and those obtained on the present report. 16	
4.3	Directivity diagram at 2kHz with CW and CCW rotation data plotted (Y-Z plane axis only). . . . .	19
4.4	Directivity diagram at 3kHz with CW and CCW rotation data plotted (Y-Z plane axis only). . . . .	20
4.5	Directivity diagram at 4kHz with CW and CCW rotation data plotted (Y-Z plane axis only). . . . .	21
B.1	DAVS hydrophone and reference hydrophone waveforms and RMS values for Y axis 1 kHz (Reson hydrophone near source) . . . . .	26
B.2	Accelerometer waveforms and RMS values for Y axis 1 kHz . . . . .	27
B.3	Accelerometer waveforms for all axis at 1 kHz . . . . .	27
B.4	DAVS hydrophone and reference hydrophone waveforms and RMS values for Y axis 2 kHz (Reson hydrophone near source) . . . . .	28
B.5	Accelerometer waveforms and RMS values for Y axis 2 kHz . . . . .	28
B.6	Accelerometer waveforms for all axis at 2 kHz . . . . .	29
B.7	DAVS hydrophone and reference hydrophone waveforms and RMS values for Y axis 3 kHz (Reson hydrophone near source) . . . . .	29
B.8	Accelerometer waveforms and RMS values for Y axis 3 kHz . . . . .	30
B.9	Accelerometer waveforms for all axis at 3 kHz . . . . .	30
B.10	DAVS hydrophone and reference hydrophone waveforms and RMS values for Y axis 4 kHz (Reson hydrophone near source) . . . . .	31
B.11	Accelerometer waveforms and RMS values for Y axis 4 kHz . . . . .	31
B.12	Accelerometer waveforms for all axis at 4 kHz . . . . .	32
B.13	DAVS hydrophone and reference hydrophone waveforms and RMS values for Z axis 0.5 kHz . . . . .	32
B.14	Accelerometer waveforms and RMS values for Z axis 0.5 kHz . . . . .	33

B.15	Accelerometer waveforms for all axis at 0.5 kHz . . . . .	33
B.16	DAVS hydrophone and reference hydrophone waveforms and RMS values for Z axis 1 kHz . . . . .	34
B.17	Accelerometer waveforms and RMS values for Z axis 1 kHz . . . . .	34
B.18	Accelerometer waveforms for all axis at 1 kHz . . . . .	35
B.19	DAVS hydrophone and reference hydrophone waveforms and RMS values for Z axis 2 kHz . . . . .	35
B.20	Accelerometer waveforms and RMS values for Z axis 2 kHz . . . . .	36
B.21	Accelerometer waveforms for all axis at 2 kHz . . . . .	36
B.22	DAVS hydrophone and reference hydrophone waveforms and RMS values for Z axis 3 kHz . . . . .	37
B.23	Accelerometer waveforms and RMS values for Z axis 3 kHz . . . . .	37
B.24	Accelerometer waveforms for all axis at 3 kHz . . . . .	38
B.25	DAVS hydrophone and reference hydrophone waveforms and RMS values for Z axis 4 kHz . . . . .	38
B.26	Accelerometer waveforms and RMS values for Z axis 4 kHz . . . . .	39
B.27	Accelerometer waveforms for all axis at 4 kHz . . . . .	39
B.28	Y axis accelerometers voltage comparison. . . . .	40
B.29	Y axis accelerometers voltage waveforms for easy comparison. Each figure represent the captured waveforms from Y axis experiment, for the 4 used frequencies. . . . .	41
B.30	Z axis accelerometers voltage comparison. . . . .	42
B.31	Z axis accelerometers voltage waveforms for easy comparison. Each figure represent the captured waveforms from Z axis experiment, for the 4 used frequencies. . . . .	43
C.1	Accelerometers directivity plot (for comparison) . . . . .	44
C.2	Accelerometers response for setup 1 CW (left) and CCW (right) at 2 kHz . . . . .	45
C.3	Accelerometer waveforms and heading information for setup 1 CW at 2 kHz . . . . .	46
C.4	Accelerometer waveforms and heading information for setup 1 CCW at 2 kHz . . . . .	46
C.5	Accelerometers response for setup 1 CW (left) and CCW (right) at 3 kHz . . . . .	47
C.6	Accelerometer waveforms and heading information for setup 1 CW at 3 kHz . . . . .	48
C.7	Accelerometer waveforms and heading information for setup 1 CCW at 3 kHz . . . . .	48
C.8	Accelerometers response for setup 1 CW (left) and CCW (right) at 4 kHz . . . . .	49
C.9	Accelerometer waveforms and heading information for setup 1 CW at 4 kHz . . . . .	50
C.10	Accelerometer waveforms and heading information for setup 1 CCW at 4 kHz . . . . .	50
C.11	Accelerometers response for setup 2 CW (left) and setup 3 CCW (right) at 2 kHz . . . . .	51
C.12	Accelerometer waveforms and heading information for setup 2 CW at 2 kHz . . . . .	52
C.13	Accelerometer waveforms and heading information for setup 3 CCW at 2 kHz . . . . .	52

# List of Tables

2.1	Time that reflections take to reach receptor transducer (propagation time for reflections, in ms). At green color the first reflection reaching transducer. The steady state zone of the direct signal at the receiver (see table 2.2) should last less than this time to avoid interferences. . . . .	4
2.2	The duration of a direct pulse (in ms), measured from the beginning of transmission to the end of reception. Cell colors represents the interferences: no overlap (white), one reflection overlapping signal (yellow), two reflections overlapping (red). . . . .	5
4.1	Files used for sensitivity calculations and obtained sensitivities and RMS voltages . . . . .	16
4.2	Files used for directivity calculations and some additional information: frequency, angles of rotation, rotation direction and setup used. . . . .	18

# Abstract

This report discusses the acoustic calibration of the Dual Accelerometer Vector Sensor (DAVS) carried out at the Arsenal do Alfeite acoustic tank, in Lisbon, on 17<sup>th</sup> and 18<sup>th</sup> of November 2016. This is a revision of previous report SiPLAB 4/17 of April 2017 [1], with a more comprehensive description of the tank limitations as well as the signal path and processing steps for obtaining calibrated curves for sensitivity and directivity in the band 0.5 to 4 kHz. Additional results from previously unprocessed data, not included in the previous report, are given for accelerometers data captured when device Z axis is pointing to the source.

# Chapter 1

## Introduction

Precise calibration of underwater acoustic devices requires relatively complex and time consuming procedures. In particular, the fact that sound speed in water is approximately five times faster than in the air, and that water impedance is low compared to most other materials, provides a setting where tank controlled tests are difficult, if not impossible, at low frequencies of interest. Depending on the tank dimensions and structure, it is common for frequencies lower than 1 kHz not to be supported. To complicate matters further, to our knowledge there are no internationally accepted standards for vector sensor hydrophones' calibration. Most procedures adopted for acoustic vector sensors are adapted or derived from pressure only hydrophone calibration experience.

The Dual Accelerometer Vector Sensor (DAVS) was developed at CINTAL during EU H2020 project WiMUST in 2016-17 [2] and tested at sea during WiMUST project wide experiments in Sines in 2017 and 2018 [3]. A preliminary DAVS calibration test was performed at the Arsenal do Alfeite facilities, in Lisbon, on 7 and 8 November 2016 [1]. The main objectives of those measurements were to obtain calibrated responses for the hydrophone and accelerometer components of the DAVS recorder and their behaviour after encapsulation into the final device. In the present report we intend to describe in higher detail the procedures taken during the test, process and show results of the data included and also other data not included in the previous report, as well as to set the limitations of the calibration procedures related to the physical characteristics of the tank, the equipment and the methodologies adopted.

This report is organized as follows: chapter 2 details the experimental tank conditions, together with equipment setup and limitations. Chapter 3 describes the signal path inside DAVS from transducer terminal up to the WAVE digital file, both for the acoustic pressure and the accelerometer sensors. This turns out to be an important step since DAVS is an integrated acquisition system, and therefore there is no direct access to the transducer output. Chapter 4 details how the results were obtained from the measurements. The used data files for sensitivity and directivity are described, for reference. The method used for sensitivity calculation is detailed and the results presented. Additional detailed plots and figures are included in the appendices. Finally, chapter 5 concludes this report and makes some considerations for future calibration experiments.

# Chapter 2

## DAVS calibration test at the Arsenal tank

The Arsenal do Alfeite is a Portuguese Navy base and harbor located in the town of Almada, in the south margin of Tagus river, just in front of Lisbon. The anechoic test tank is a facility located inside the base and comprises a 8 m long by 5 m wide and a 5 m deep basin, fully equipped with remote controlled sliding bridges and dry wells for equipment testing and installation. In our case, the reference comparison method was used. Data was acquired from DAVS and from two reference Reson TC4033-6 hydrophones for further analysis. The next sections present an overview of the tests performed and additional information about the tank itself.

### 2.1 Theoretic propagation times for the Arsenal tank

An important piece of information is the limitations imposed by the physical characteristics of the tank itself due to acoustic reflections on the lateral walls bottom and surface. The theoretical propagation times were calculated for the experiments to be carried out, and considering the dimensions of the tank. This calculations followed the method described in report [4].

For receiving transducers at mid tank depth, and the projector at a distance of 2 m from the wall, the propagation time was calculated for source-emitter distances of 0.5, 1, 2, 3, 4, 5 and 6 m, as shown in figure 2.1. Then, for several combinations of frequency and pulse length, the pulse duration was found and added to the direct propagation time. This is the time that a complete pulse takes from the emission till the end of reception, and any reflection should take longer than that time in order to avoid interference. For the Arsenal tank it was found that for frequencies lower than 1 kHz it is impossible to avoid interference. Table 2.1 shows the time for the reflections to get to the receiver. Table 2.2 shows the obtained values, for some frequencies and pulse lenght. The duration column represents the pulse duration in ms for that frequency and number of cycles. Then, the distance between transducers columns represents the pulse duration plus the propagation duration, for the distances (0.5 to 7 m). The yellow cells denote at least one reflection overlap and the red cells are those with more than one propagation path overlap. It is important to note that the tank walls are covered all around with anechoic panels that absorb the acoustic waves and minimize reverberation but, of course, do not completely

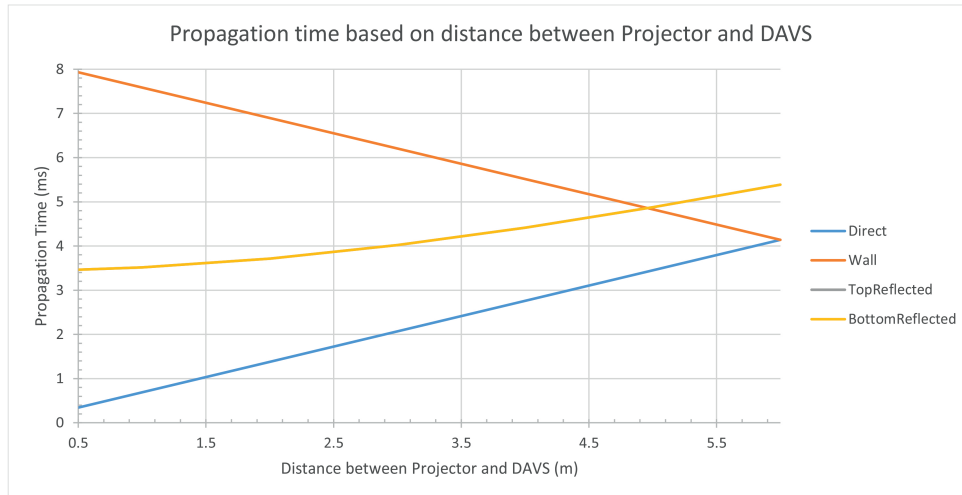


Figure 2.1: Theoretical propagation times for the Arsenal tank, with transducers at mid depth and various source - receiver distances (X axis). Note that the top and bottom reflected times are overlapped.

Distance between transducers (m)	0.5	1	2	3	4	5	6	7
Wall reflected propagation time (ms)	7.931	7.5862	6.8966	6.2069	5.5172	4.8276	4.1379	3.4483
Top/Bottom reflected time (ms)	3.4655	3.5166	3.7139	4.0213	4.4159	4.8766	5.3864	5.9326

Table 2.1: Time that reflections take to reach receptor transducer (propagation time for reflections, in ms). At green color the first reflection reaching transducer. The steady state zone of the direct signal at the receiver (see table 2.2) should last less than this time to avoid interferences.

eliminate all reflected energy. This reverberation may be highly attenuated, and in some cases where the direct path overlaps with one reflection, the resulting signal can still be used to provide a relatively error free measurement. However, for lower frequencies, we must always take into account that interference exists and can negatively influence the precision of the calculations. As expected, for lower distances between transducers there is a larger free reflection time window. This will also depend on the signal pulse length, which contributes for reducing the affordable reflection free time window. Since the shorter distances can also affect the wave front shape (from plane wave to spherical) and therefore the far field condition, the distance of 2 and 3 m were chosen for the case of the Arsenal tank. The required pulse length was only evaluated during the experiment, since it largely depends on the available equipment, and the transient response time it can achieve.

## 2.2 DAVS sensitivity test

To determine the DAVS sensitivity, two experiments were performed while changing the DAVS direction plane pointing to source. The DAVS directions respect the accelerometer axis, for example, the X axis experiments correspond to the positive X axis of accelerometer. During the afternoon of the first day, several measurements were done pointing DAVS Z axis (Z-Y plane) to the projector at 3 m, as represented in figure 2.2. The used projector is the Sensortech SX05 dogbone, connected to an amplifier (Sensortech SS21) and to a signal generator (Agilent 33120A). Several pulse lengths were tested but it was

Freq. (Hz)	Pulse cycles	Duration (ms)	Distance between transducers (m)							
			0.5	1	2	3	4	5	6	7
500	5.00	10.00	10.34	10.69	11.38	12.07	12.76	13.45	14.14	14.83
500	10.00	20.00	20.34	20.69	21.38	22.07	22.76	23.45	24.14	24.83
500	15.00	30.00	30.34	30.69	31.38	32.07	32.76	33.45	34.14	34.83
500	20.00	40.00	40.34	40.69	41.38	42.07	42.76	43.45	44.14	44.83
1000	5.00	5.00	5.34	5.69	6.38	7.07	7.76	8.45	9.14	9.83
1000	10.00	10.00	10.34	10.69	11.38	12.07	12.76	13.45	14.14	14.83
1000	15.00	15.00	15.34	15.69	16.38	17.07	17.76	18.45	19.14	19.83
1000	20.00	20.00	20.34	20.69	21.38	22.07	22.76	23.45	24.14	24.83
2000	5.00	2.50	2.84	3.19	3.88	4.57	5.26	5.95	6.64	7.33
2000	10.00	5.00	5.34	5.69	6.38	7.07	7.76	8.45	9.14	9.83
2000	15.00	7.50	7.84	8.19	8.88	9.57	10.26	10.95	11.64	12.33
2000	20.00	10.00	10.34	10.69	11.38	12.07	12.76	13.45	14.14	14.83
3000	5.00	1.67	2.01	2.36	3.05	3.74	4.43	5.11	5.80	6.49
3000	10.00	3.33	3.68	4.02	4.71	5.40	6.09	6.78	7.47	8.16
3000	15.00	5.00	5.34	5.69	6.38	7.07	7.76	8.45	9.14	9.83
3000	20.00	6.67	7.01	7.36	8.05	8.74	9.43	10.11	10.80	11.49
4000	5.00	1.25	1.59	1.94	2.63	3.32	4.01	4.70	5.39	6.08
4000	10.00	2.50	2.84	3.19	3.88	4.57	5.26	5.95	6.64	7.33
4000	15.00	3.75	4.09	4.44	5.13	5.82	6.51	7.20	7.89	8.58
4000	20.00	5.00	5.34	5.69	6.38	7.07	7.76	8.45	9.14	9.83
5000	5.00	1.00	1.34	1.69	2.38	3.07	3.76	4.45	5.14	5.83
5000	10.00	2.00	2.34	2.69	3.38	4.07	4.76	5.45	6.14	6.83
5000	15.00	3.00	3.34	3.69	4.38	5.07	5.76	6.45	7.14	7.83
5000	20.00	4.00	4.34	4.69	5.38	6.07	6.76	7.45	8.14	8.83

Table 2.2: The duration of a direct pulse (in ms), measured from the beginning of transmission to the end of reception. Cell colors represents the interferences: no overlap (white), one reflection overlapping signal (yellow), two reflections overlapping (red).

experimentally determined that 20 cycles were a reasonable value. The frequencies used for the tone signals were 0.5, 1, 2, 3 and 4 kHz. Two reference Reson TC4033-6 hydrophones were used: one at 1 m of the source and the other at 0.5 m of DAVS. These two hydrophones have a receiving sensitivity of  $-202 \text{ dB}/\text{V}/\mu\text{Pa}$  for the used frequency range. An additional B&K hydrophone, part of the tank equipment, was also placed near DAVS. All devices were placed at the same depth of 2.5 m, in the middle of the tank. To capture the reference hydrophones output an Agilent oscilloscope (MSO-X 3014A) was used and some pulse waveforms captured and stored on a USB pen. DAVS base station in streaming mode (see user manual [5]) was used and data saved in WAVE files.

During the second day another group of 10 measurements was performed, using a similar setup as that for the Z axis but with DAVS Y axis pointing to source, as shown in figure 2.3. Tone signals of 0.5, 1, 2, 3 and 4 kHz and changing the pulse length between 20 and 25 cycles, for each frequency setting were transmitted. However, in this second day, the reference hydrophone near DAVS was removed, since it was noticed that it could be causing some interference. Only the Reson for monitoring the source emitted signal was kept in place. After the experiment, just the 20 cycles pulse length was used for the analysis, since it provided enough steady state cycles for detection and estimation.

The oscilloscope captured one complete pulse and stored the data onto a \*.csv format file, that contains the 3 input channels and the capture times. This file has at least 2 columns, the first column is the capture time and the other columns the captured channels. The used channels are identified in the first line of the file, the header line, since the capture can have only 1, 2 or 3 channels. The second line has the units used, which is seconds for the time data and Volt for the acquired signals. During the experiment the Reson near DAVS was plugged to channel 1, the Reson near source was acquired on channel 2 and the B&K model on channel 3.

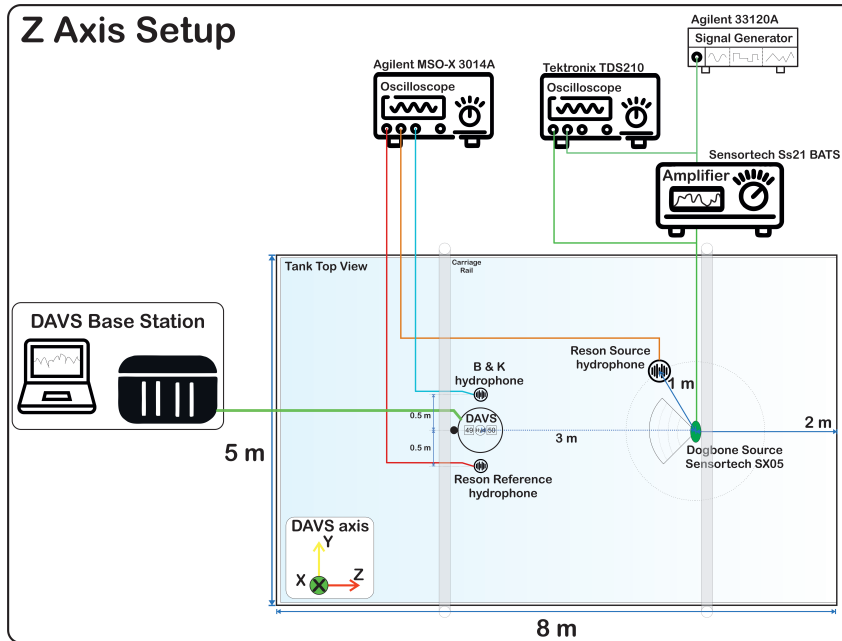


Figure 2.2: Sensitivity experiment setup for Z axis test.

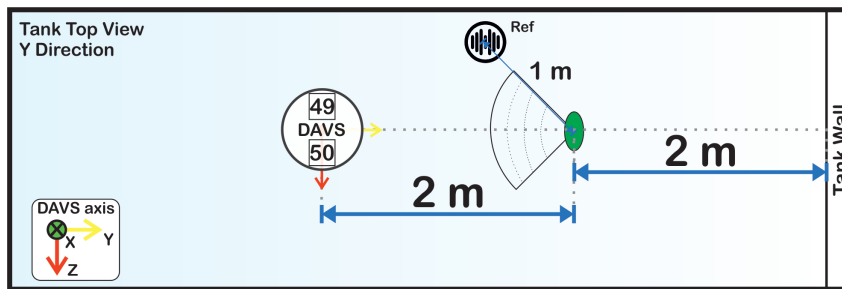


Figure 2.3: Setup placement for Y axis sensitivity experiment.

## 2.3 DAVS directivity test

During the second day a directivity test was carried out using the configuration shown in figure 2.4. Tone bursts at 2, 3 and 4 kHz were used with the DAVS rotated in the Z-Y plane and the data of a full 360 degrees turn was acquired and stored. Additionally, the heading information from the DAVS internal electronic compass was also acquired and stored. During these tests, alternative setups were used to check if the setup arrangement had influence/interference in the captured signals:

1. in setup 1 DAVS was placed at 3 m from source, and the source was at 2 m of tank wall. The attachment used was a short rod.
2. in setup 2 DAVS was placed at 2 m from source, and the source was at 3 m of tank wall. The attachment used was a long rod.
3. in setup 3 DAVS was placed at 3 m from source, and the source was at 2 m of tank wall. The attachment used was a long rod.

However, in the end setup 1 was chosen for the test. For these experiments no reference hydrophone was used.

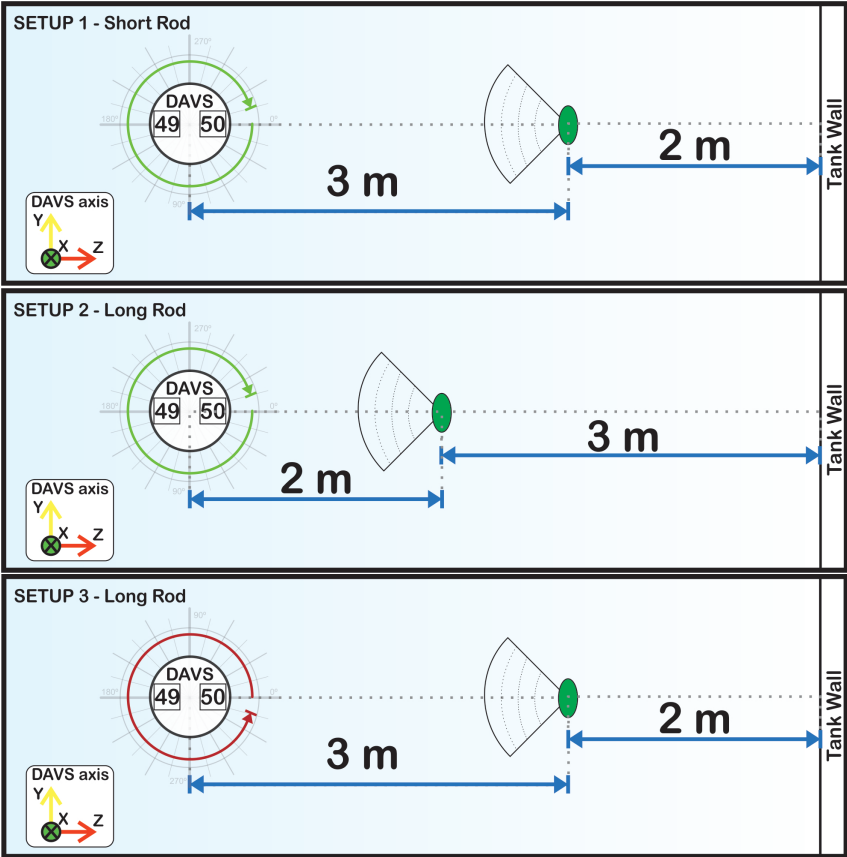


Figure 2.4: Three setups and placement of devices used for directivity measurements. Note that the clockwise and then the counter clockwise rotation were used for the experiments.

# Chapter 3

## DAVS signal path

Since the DAVS is a complete acquisition system there is no direct access to transducer terminals to obtain the voltages and make comparisons with the reference hydrophone. We must convert the output WAVE file values back to the voltage at transducer output, before performing the sensitivity calculation. In order to do so we need to know the exact signal path from the transducers' output to the stored WAVE file and which modifications the signal suffer through this path. The path is different depending on whether the accelerometer or the hydrophone are being used. The following sections will detail each of the signals' path and the conversions performed in order to obtain the input real physical quantity. More information about DAVS hardware can be found on report [5].

### 3.1 DAVS hydrophone forward and backward signal path

The hydrophone signal path (figure 3.1) starts at the hydrophone input where the incident sound pressure waves are transformed onto an electrical voltage. This voltage will go through a pre-amplifier with a fixed gain of 39, followed by a user programmable gain amplifier (PGA), with output ranges from -5 to 5 volt. Depending on the user selected gain from the available options (1x, 2x, 4x, 8x, 16x, 32x or 64x), the signal gets amplified and forwarded to a single ended to differential output circuit, which is responsible for adapting the output ranges of the PGA ( $\pm 5\text{ V}$ ) to the input ranges of the analog to digital ADC converter (0-5 V). By using a differential input, the ADC require that 2 signals are used to represent the original signal we want to digitize. These signals will be 2 opposite signals, whose amplitudes are symmetrical around some reference value. The single ended to differential circuit creates these 2 signals from the PGA signal by dividing it by two and adding an offset of 2.5 Volt. This way, the differential signals will oscillate around 2.5 V and the extreme values will be 0 and 5 V, the maximum electrical ranges of the ADC input. This corresponds to an input range of  $\pm 2.5\text{ Volt}$ , considering that both signals will oscillate around the 2.5 V offset. The output of ADC, a digital signal, is then saved into a WAVE file by the micro-controller. The plain reading of the WAVE file gives us normalized values in the range  $\pm 1\text{ Volt}$ . Therefore, since the input range of the ADC is  $\pm 2.5\text{ Volt}$  and the normalized output is  $\pm 1\text{ Volt}$ , the gain factor is  $1/2.5 = 0.4$ . To simplify the math, the single ended and ADC gains are expressed together as a division by 5 or a gain of 0.2x ( $0.5*0.4 = 0.2x$ ) and called through this text ADC sensitivity. The selected PGA gain is obtained from the WAVE file header, which stores

this information. To explain the total hydrophone path we will present the various steps of the signal passing through each component.

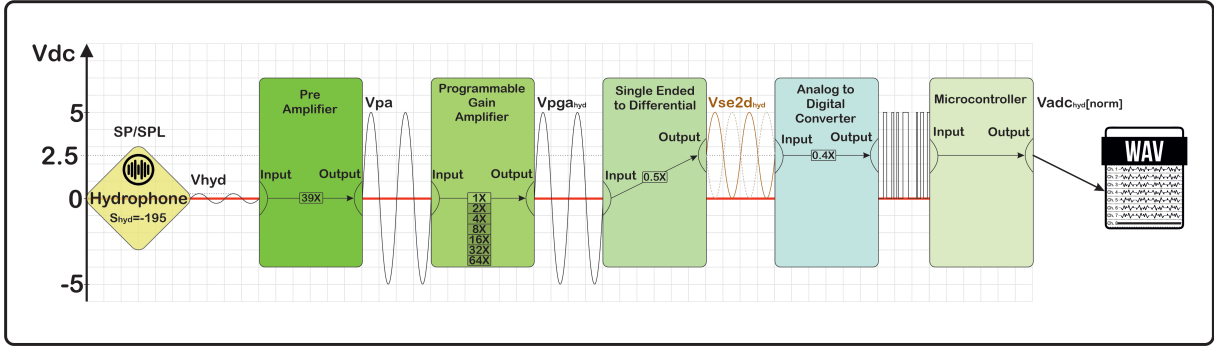


Figure 3.1: DAVS hydrophone signal path: from sensor (left) to digital WAVE file (right).

### 3.1.1 Voltage at hydrophone terminals

The voltage  $V_{hyd}$  is usually referred as Open Circuit Receiving Response (OCRR) or Open Circuit Voltage (OCV). The OCRR/OCV is the voltage generated by the transducer with no output current, per  $\mu\text{Pa}$  of sound pressure applied and its input as a function of frequency. It's commonly referred to 1 Volt [dB re 1V].

$$V_{hyd}[\text{dB re 1V}] = 20 * \log_{10}\left(\frac{V_{hyd}}{1[\text{V}]}\right) = 20 * \log_{10}(V_{hyd}[\text{V}]). \quad (3.1)$$

This  $V_{hyd}$  [V] is the root mean square (rms) voltage, that is the peak to peak voltage  $V_{hyd_{p2p}}$  divided by twice the square root of 2:

$$V_{hyd}[\text{V}] = \frac{V_{hyd_{p2p}}}{2 * \sqrt{2}}. \quad (3.2)$$

When directly measuring the hydrophone output voltage with an oscilloscope, the peak voltage is an easy and practical value to read. However, we don't have direct access to DAVS hydrophone terminals, so this value must be obtained from the raw WAVE output data. This voltage is related to incident sound pressure and hydrophone sensitivity (please see appendix A.1 for additional information).

### 3.1.2 DAVS hydrophone pre-amplifier gain

The purpose of the pre-amplifier stage is to amplify the very weak signal from the output terminals of the hydrophone. The DAVS has a fixed gain of 39x (or 31.82 dB) at the pre-amplifier stage. The output voltage of the pre-amplifier  $V_{pa}$  will then be:

$$V_{pa}[\text{V}] = V_{hyd}[\text{V}] * 39. \quad (3.3)$$

If we are working with decibel units and have the voltage at hydrophone terminals, (3.3) becomes

$$V_{pa}[\text{dB}] = 20\log(V_{hyd}[\text{V}]) + 31.82. \quad (3.4)$$

### 3.1.3 DAVS hydrophone programmable gain amplifier (PGA)

The PGA is the stage that follows the pre-amplifier, and here the gain value  $G_{\text{pga}_{\text{hyd}}}$  is selected by the user and can be retrieved from the WAVE file header. The following options are available: 1x, 2x, 4x, 8x, 16x, 32x or 64x. In a similar way as for the pre-amplifier, the PGA output  $V_{\text{pga}_{\text{hyd}}}$  [V] is given by

$$V_{\text{pga}_{\text{hyd}}}[\text{V}] = V_{\text{pa}}[\text{V}] * G_{\text{pga}_{\text{hyd}}}. \quad (3.5)$$

In a dB scale  $V_{\text{pga}_{\text{hyd}}}$  will be the output of pre-amplifier  $V_{\text{pa}}$  plus the selected gain of PGA  $G_{\text{pga}_{\text{hyd}}}$  in dB units:

$$V_{\text{pga}_{\text{hyd}}}[\text{dB}] = V_{\text{pa}}[\text{dB}] + G_{\text{pga}_{\text{hyd}}}[\text{dB}], \quad (3.6)$$

where  $G_{\text{pga}_{\text{hyd}}}$  [dB] takes the values 0, 6, 12, 18, 24, 30 or 36 dB.

### 3.1.4 DAVS hydrophone single ended to differential

The single ended to differential circuit adapts the amplitude of the signal by reducing the PGA output  $V_{\text{pga}_{\text{hyd}}}$  by a factor of 2, thus

$$V_{\text{se2d}_{\text{hyd}}}[\text{V}] = V_{\text{pga}_{\text{hyd}}}[\text{V}] * 0.5. \quad (3.7)$$

In a dB scale this reduction corresponds to subtracting 6 dB from the  $V_{\text{pga}_{\text{hyd}}}$  output value (also in dB), thus

$$V_{\text{se2d}_{\text{hyd}}}[\text{dB}] = V_{\text{pga}_{\text{hyd}}}[\text{dB}] - 6[\text{dB}]. \quad (3.8)$$

Additionally, it adds an offset voltage of 2.5 Volt, but that operation does not affects the signal amplitude.

### 3.1.5 DAVS hydrophone ADC / WAVE file

As explained in the previous section, the Analog to Digital Converter (ADC) does not changes signal amplitude, but the digital data format of the WAVE file is normalized so the ADC input signal excursion of  $\pm 2.5$  Volt is to be taken into account. So, it is considered that the output of the single ended to differential circuit  $V_{\text{se2d}_{\text{hyd}}}$  is divided by 2.5 (or multiplied by 0.4) when passing through the ADC to obtain the normalized WAVE data  $WAVE_{V_{\text{hyd}}}$ :

$$WAVE_{V_{\text{hyd}}} = V_{\text{se2d}_{\text{hyd}}}[\text{V}] * 0.4. \quad (3.9)$$

Note that we did not consider the digital value obtained at the output of ADC (the raw digital sample present at WAVE file) but the converted float value from that digital sample, which is normalized between -1 and 1. This is the value that we have when opening the WAVE file in a software like Matlab.

In a dB scale, this reduction corresponds to subtracting -7.96 dB from the  $V_{\text{se2d}_{\text{hyd}}}$  output value, as:

$$WAVE_{V_{\text{hyd}}}[\text{dB}] = V_{\text{se2d}_{\text{hyd}}}[\text{dB}] - 7.96[\text{dB}] \quad (3.10)$$

Note that values from Matlab/WAVE file are in linear units and need to be converted to a dB scale.

### 3.1.6 DAVS hydrophone full forward and backward path

Joining all steps above into one single end to end formula, based on the hydrophone OCR voltage  $V_{\text{hyd}}$  and the user selected gain of PGA  $G_{\text{pga}_{\text{hyd}}}$ :

$$WAVE_{V_{\text{hyd}}} = V_{\text{hyd}}[\text{V}] * 39 * G_{\text{pga}_{\text{hyd}}} * 0.5 * 0.4 = V_{\text{hyd}}[\text{V}] * G_{\text{pga}_{\text{hyd}}} * 7.8. \quad (3.11)$$

To convert the normalized values from a DAVS WAVE file  $WAVE_{V_{\text{hyd}}}$  into the voltage at the hydrophone terminals  $V_{\text{hyd}}$ , we can use (3.11) which simplify as:

$$V_{\text{hyd}}[\text{V}] = \frac{WAVE_{V_{\text{hyd}}}}{G_{\text{pga}_{\text{hyd}}} * 7.8}. \quad (3.12)$$

This last formula is the one that we will use to get the hydrophone OCR voltage and calculate the sensitivity.

When using a logarithmic scale, (3.11) turns into:

$$\begin{aligned} WAVE_{V_{\text{hyd}}}[\text{dB}] &= 20\log(V_{\text{hyd}}[\text{V}]) + 31.82 + G_{\text{pga}_{\text{hyd}}}[\text{dB}] - 6 - 7.96, \\ &= 20\log(V_{\text{hyd}}[\text{V}]) + G_{\text{pga}_{\text{hyd}}}[\text{dB}] + 17.86. \end{aligned} \quad (3.13)$$

The hydrophone voltage can be obtained from (3.12) with:

$$20\log(V_{\text{hyd}}[\text{V}]) = WAVE_{V_{\text{hyd}}} - G_{\text{pga}_{\text{hyd}}}[\text{dB}] - 17.86, \quad (3.14)$$

$$V_{\text{hyd}}[\text{V}] = 10^{\frac{WAVE_{V_{\text{hyd}}} - G_{\text{pga}_{\text{hyd}}}[\text{dB}] - 17.86}{20}}. \quad (3.15)$$

## 3.2 DAVS accelerometer forward and backward signal path

The accelerometer forward signal path shown in figure 3.2, starts at the voltage output of the IEPE power source, which ranges between  $\pm 5$  Volt, and then goes through a number of steps, besides the pre-amplifier, all the same as for the hydrophone: the PGA, the single to differential converter and the ADC. Then the signal is digitised and saved to a WAVE file by the micro-controller, exactly as for the hydrophone channel.

### 3.2.1 Accelerometer sensitivity

The accelerometer sensitivity is given by the formula that relates the voltage output at its terminals and the acceleration applied along some axis X,Y or Z:

$$S_{\text{acc}} = \frac{V_{\text{acc}}}{A_{\text{acc}}} \left[ \frac{\text{V}}{\text{m/s}^2} \right]. \quad (3.16)$$

The accelerometer sensitivity is given by the manufacturer as 51 mV/(m/s<sup>2</sup>), corresponding to the output voltage for an acceleration of 1 m/s<sup>2</sup>. This sensitivity is frequency

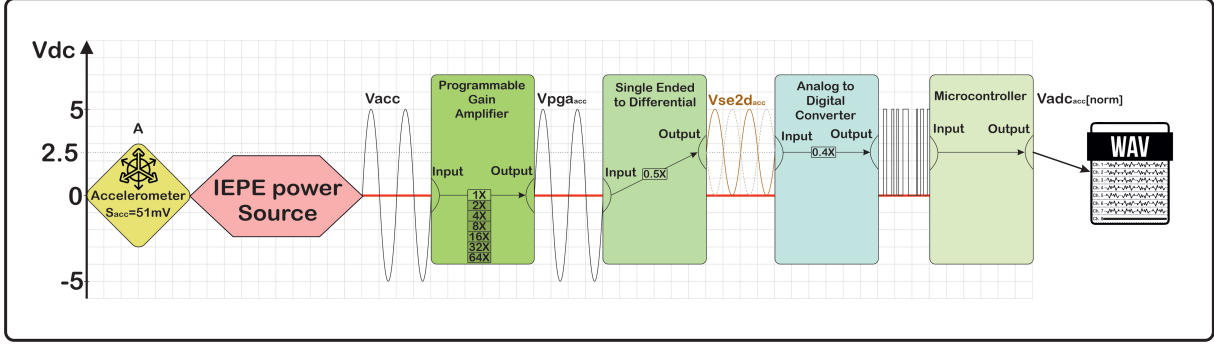


Figure 3.2: Accelerometer signal path: the accelerometer (left) to the digital WAVE file (right).

dependent and may vary, according to the manufacturer, within  $\pm 10\%$  ( $\pm 5.1$  mV) in the frequency range of 500 Hz to 4 kHz. It is important to note that this sensitivity is the value from manufacturer for the individual devices, used in air without any encapsulation. In the DAVS system the accelerometers are assembled in a polyurethane structure and attached to the DAVS cylinder with all the electronics. These structures and the underwater deployment may significantly change the frequency response of the device, thus the need to calibrate the complete device and determine reference values.

### 3.2.2 DAVS accelerometer PGA, single ended to differential and ADC/WAVE file

The signal path from the output of IEPE power source  $V_{acc}$  will be equal to that of the output of the hydrophone pre-amplifier, so the formulas used for that case will be similar:

$$V_{pga_{acc}} [V] = V_{acc} [V] * G_{pga_{acc}}, \quad (3.17)$$

$$V_{se2d_{acc}} [V] = V_{pga_{acc}} [V] * 0.5, \quad (3.18)$$

$$WAVE_{V_{acc}} = V_{se2d_{acc}} [V] * 0.4. \quad (3.19)$$

### 3.2.3 DAVS Accelerometer full forward and backward path

Joining all linear formulas into one single formula, based on accelerometer output voltage  $V_{acc}$  and the user selected gain of PGA  $G_{pga_{acc}}$ :

$$WAVE_{V_{acc}} = V_{acc} [V] * G_{pga_{acc}} * 0.5 * 0.4 = V_{acc} [V] * G_{pga_{acc}} * 0.2. \quad (3.20)$$

To convert the normalized WAVE file values  $WAVE_{V_{acc}}$  into a voltage at accelerometer terminals  $V_{acc}$  we use:

$$V_{acc} [V] = \frac{WAVE_{V_{acc}}}{G_{pga_{acc}} * 0.2}. \quad (3.21)$$

This last formula is based on the accelerometer PGA gain, retrieved from WAVE file header.

In dB scale:

$$\begin{aligned} WAVE_{V_{acc}} [dB] &= 20 \log(V_{acc} [V]) + G_{pga_{acc}} - 6 - 7.96, \\ &= 20 \log(V_{acc} [V]) + G_{pga_{acc}} - 13.96. \end{aligned} \quad (3.22)$$

$$V_{\text{acc}}[\text{V}] = 10^{\frac{WAVE_{V_{\text{acc}}} - G_{\text{pgaacc}} + 13.96}{20}}. \quad (3.23)$$

Remember that  $WAVE_{V_{\text{acc}}}$  is obtained from a software reader, such as a Matlab, and values are in linear scale.

# Chapter 4

## DAVS Calibration - Data Processing

DAVS calibration is obtained thanks to reading the data files containing the WAVE output, the compass data and the oscilloscope output information. For each test the required files were grouped into a folder and a Matlab script created to process each WAVE file. Below are the details on how the files were processed and the results obtained for the analysis of the sensitivity and the directivity.

### 4.1 DAVS sensitivity analysis methodology

To obtain the hydrophone and accelerometer sensitivities, the following sequence takes place:

1. The first step is to convert WAVE channel data into voltages at respective transducer terminals using (3.12) and (3.21):

$$V_{\text{hyd}}[\mathbf{V}] = \frac{WAVE_{V_{\text{hyd}}}}{G_{\text{pga}_{\text{hyd}}} * 0.2}, \quad (4.1)$$

$$V_{\text{acc}}[\mathbf{V}] = \frac{WAVE_{V_{\text{acc}}}}{G_{\text{pga}_{\text{acc}}} * 8}, \quad (4.2)$$

for the pressure hydrophone and the accelerometers, respectively. These equations use the PGA gains read from the WAVE file header.

2. The first pulse is isolated from the complete WAVE data and band passed between 500 and 5 kHz. The choice of the first pulse was a personal option but could have been any other, since they must be similar.
3. The reference hydrophones' data is loaded from the oscilloscope \*.csv file. The data from Reson, the one near DAVS or that near the source, are also filtered (depending on Z or Y experiment). 20 peaks corresponding to the emitted pulse are identified. The first ones are discarded, which correspond to initial transient zone. During this work we discard the first 5 (Y axis) or 7 (Z axis). Then, the following 9 peaks (Y axis) or 11 peaks (Z value) are used to determine the RMS voltage ( $V_{\text{RMS}_{\text{ref}}}$ ). These peaks are averaged before RMS calculation. The last peaks are not used to minimize disturbances caused by the reflections of the tank.

4. From the DAVS hydrophone data 20 peaks are also identified, discarding the first ones and finding the RMS from the following peaks average value ( $V_{\text{RMS}_{\text{hyd}}}$ ). The initial peak and the peak quantity are the same used for the reference hydrophone.
5. The DAVS hydrophone sensitivity can now be obtained from these RMS values ( $V_{\text{RMS}_{\text{hyd}}}$  and  $V_{\text{RMS}_{\text{ref}}}$ ), considering the reference Reson sensitivity  $S_{\text{ref}}$  (-202 dB re 1V/ $\mu$ Pa):

$$S_{\text{hyd}} = S_{\text{ref}} + 20\log_{10}(V_{\text{RMS}_{\text{hyd}}}) - 20\log_{10}(V_{\text{RMS}_{\text{ref}}}). \quad (4.3)$$

6. For the Y Axis orientation, the reference Reson hydrophone near DAVS was removed and only the source Reson was used as the reference hydrophone. A distance of 2 m separate the source and DAVS, so in this case the hydrophone sensitivity formula used is [dB]:

$$S_{\text{hyd}} = S_{\text{ref}} + 20\log_{10}(V_{\text{RMS}_{\text{hyd}}}) - 20\log_{10}(V_{\text{RMS}_{\text{ref}}}) + 20\log_{10}(2). \quad (4.4)$$

7. For the acceleration sensitivity the same pulse of the front axis data (the axis pointing to source Y or Z) was isolated from the two accelerometer. The same 20 peaks are found, the first 6 discarded and the following 10 averaged and root mean squared.
8. The accelerometer sensitivity is obtained by relating the reference hydrophone output with the accelerometer output. This relation is called pressure equivalent sensitivity  $S_{\text{peq}}$  and is based on accelerometer voltage  $V_{\text{RMS}_{\text{acc}}}$ , reference hydrophone RMS voltage  $V_{\text{RMS}_{\text{ref}}}$  and reference hydrophone sensitivity  $S_{\text{ref}}$  [dB]:

$$S_{\text{peq}} = S_{\text{ref}} + 20\log_{10}(V_{\text{RMS}_{\text{acc}}}) - 20\log_{10}(V_{\text{RMS}_{\text{ref}}}). \quad (4.5)$$

The obtained value is then linearised and referred to  $\mu$ Pa units:

$$M_p = 10^{\frac{S_{\text{peq}}}{20}} * 10^6. \quad (4.6)$$

9. Finally the accelerometer sensitivity  $M_a$  is obtained through the relation of the acoustic impedance  $\rho c$  and the frequency of the pulse signal  $f$ , with the pressure equivalent sensitivity  $M_p$  (water density  $\rho$ , depending on the test site but near 1026  $kg/m^3$ ; speed of wave in water  $c$ , around 1500  $m/s$ ):

$$M_a = \frac{\rho c}{\omega} * M_p = \frac{\rho c}{2\pi f} * M_p. \quad (4.7)$$

10. Several graphs are plotted with different measurements of DAVS hydrophones, accelerometers and reference hydrophones.

## 4.2 DAVS sensitivity analysis

For the sensitivity calculation the data files described in table 4.1, were chosen and processed. The Y axis files are the same used on report [1], while the first 5 Z axis files were not previously analysed and are give in the present report, besides last Z axis file (313105107) that was also used on report [1]. Table 4.1 shows the results obtained both for transducer sensitivities and the voltages found at transducers terminals. Figure 4.1 shows the sensitivities obtained for the hydrophone (left) and the two accelerometers (right). All the waveforms are in appendix B, for reference.

WAVE filename	Scope filename	f kHz	Axis (front)	Hyd S dB re V/uPa	Acc49 S mV/ms-1	Acc50 S mV/ms-1	Reson RMS mV	Hyd RMS mV	Acc49 RMS mV	Acc50 Rms mV
312160624	Scope 15	0.5	Z	-195.39	1.12	1.50	0.118	0.25238	0.02042	0.027358
312155633	Scope 12	1	Z	-197.66	10.79	8.43	0.7281	1.1586	1.1691	0.9133
312155118	Scope 11	2	Z	-187.32*	57.92	41.02	0.2109*	1.1431	1.8831	1.3337
312153528	Scope 9	3	Z	-194.61	53.75	48.63	0.9557	2.2371	7.9201	7.1663
312152440	Scope 8	4	Z	-194.94	35.73	87.30	0.8039	1.8128	4.4292	10.8204
313135255	Scope 14	1	Y	-196.95	27.64	27.26	0.9616	0.85964	1.3658	1.3473
313135817	Scope 16	2	Y	-197.75	13.14	13.59	1.9384	1.5801	2.6185	2.708
313140331	Scope 18	3	Y	-194.99	15.89	16.12	4.9266	5.5224	12.0738	12.247
313141019	Scope 20	4	Y	-195.04	17.99	18.79	2.2672	2.5251	8.3859	8.7594
313105107	Scope 9	3	Z	-196.40	36.97	38.05	1.6318	3.1094	9.3011	9.6872

Table 4.1: Files used for sensitivity calculations and obtained sensitivities and RMS voltages

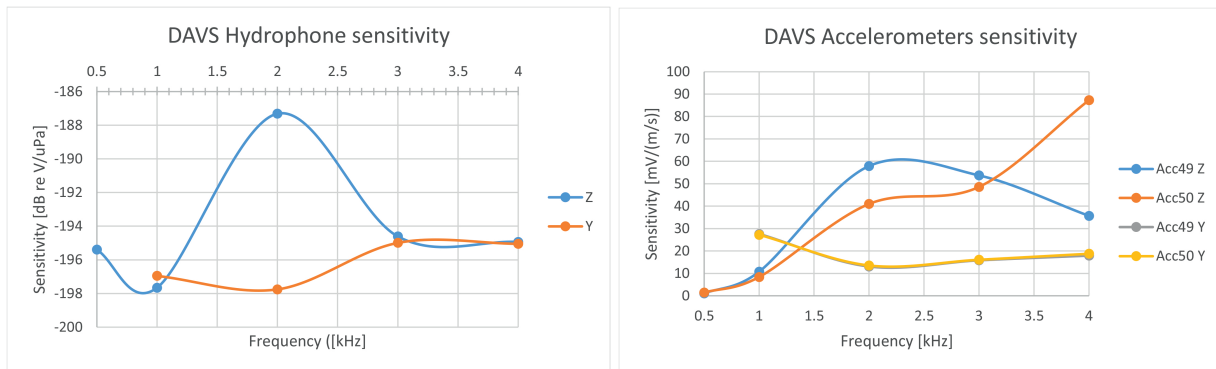


Figure 4.1: Obtained hydrophone (left graph) and accelerometer sensitivities (right graph), for the 2 used orientations (Y and Z pointing to source)

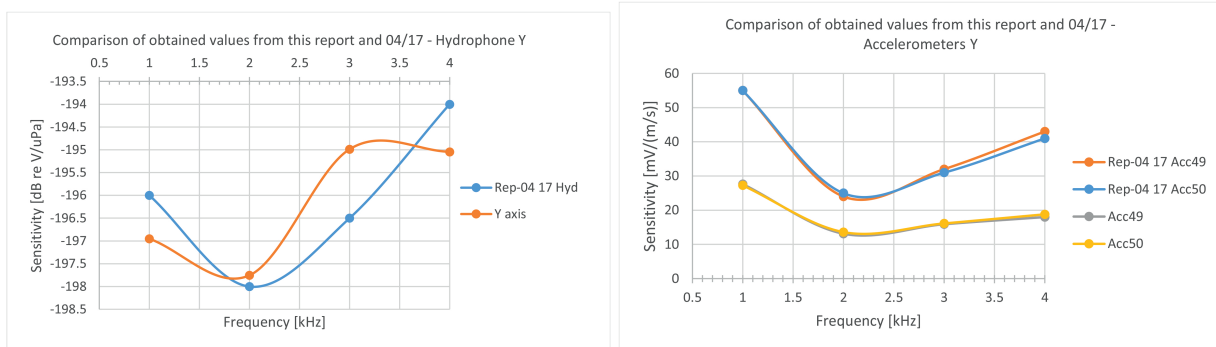


Figure 4.2: Comparison of sensor sensitivities (Y axis pointing to source) between values obtained in the report [1] and those obtained on the present report.

For the 500 Hz Z axis test case, the DAVS and reference signal were very weak compared to the other frequencies (approximately 1.5 mV as can be seen in figure B.13). A band pass filter with cutoff frequencies from 300 to 700 Hz was used only on this case, to try to recover the signal. The accelerometer waveforms can be seen on figure B.15 that shows the Z axis with a lower amplitude than the X axis (0.04 mV for Z and 0.16 mV for X).

For 1 kHz, the hydrophone signal is stable at Z axis test (B.16) but present some interference on Y axis test B.1. These shape variations are the result of the reverberant signals coming from the tank boundaries. When looking at accelerometer waveforms of Z experiment (figure B.18) it can be noticed that all components have the same order of amplitudes and a strong noise component changing its shape. For the Y axis, the differences are more subtle, but are also present (figure B.3).

For the 2 KHz Z axis test, there was also some noise in the capture of reference hydrophone (figure B.19), so the obtained sensitivity is not correct. When using the Reson hydrophone positioned near the sound source as reference, a gain of -200 dB was obtained, which appears to be a more correct value. When looking at accelerometer waveforms a noise component can also be noticed. This may have been due to some interference problem specific to the facilities at the Arsenal so this measurement should be repeated.

The hydrophone signals for 3 kHz present a relatively stable signal (figures B.7 and B.22). The accelerometers Z axis experiment waveforms shows that Z axis have the same amplitude and the X/Y axis are around 1/3 of that value (figure B.24). The Y axis test present an Z axis amplitude very close to Y in the accelerometer #49 (figure B.9).

The 4 kHz experiment show that the hydrophone signal follows the expected shape with minor variation, as seen on figures B.10 and B.25. However, accelerometer #49 for Z axis experiment, has a peak amplitude that is near half of the peak amplitude of accelerometer #50 (figures B.26 and B.27). The other axis of accelerometer #49 also has a higher amplitude, near half that of the Z axis. This does not happen for accelerometer #50.

### 4.3 DAVS directivity analysis methodology

To find the directivity plots each WAVE file were processed into Matlab along the following steps:

1. Load WAVE file and retrieve date and time of acquisition, creating time arrays.
2. Load heading information from "Compass\_dddhhmmss.csv" filtering the beginning and the ending of rotation angles, times and indexes.
3. Process accelerometer channels by band passing them, finding peaks envelope, normalize envelope with the maximum channel value and convert it to dB scale.
4. Isolate only the full rotation data from each logarithmic data arrays.
5. Rotate arrays to adjust polar plot axis to arrays. 0 degrees in polar plots are the start of rotation, where the positive angles are corresponding to when the rotation was in clockwise direction. When a counter clockwise direction file is used, the rotation follow the negative scale, starting at 0 degrees and following the negative values.
6. Plot polar graphs with Y and Z axis.

The processing is fully automated, but some settings can be fine-tuned for the peak values or for the rotation detection. For the rotation detection, it is known that the support platform rotation speed is approximately 1.4 degrees per second and the compass sample rate is 1 Hz. To automate the detection of rotation start we look at the heading angles stored in compass file. When adjacent compass file samples have a angle difference less than 1 degree, its assumed that DAVS is not rotating. When this difference is larger than 1 degree, DAVS is rotating. It is possible to use a value around 1.4 degrees per second, which is the rotation speed of the support platform, however 1 degree was chosen because it is a nice compromise between the compass noise and the rotation start detection. After start rotating, the support platform stop only after a full rotation was done. So, we detect the end of rotation when the difference of adjacent samples is again less than 1.

## 4.4 DAVS directivity analysis

For the directivity tests, table 4.2 shows the used files and some specific information. For each file a directional plot was obtained per each accelerometer axis, as can be seen in appendix C. To better compare the directional response, the files with the same frequency were overlapped in the same plot, as seen in the following sections. The files from setups 2 and 3 were ignored from this comparison, since they have incomplete rotation or no differences were found from setup 1. The hydrophone and X axis data were not used. To simplify the comparison, figure C.1 in appendix, where the 3 frequency experiments are plotted in the same figure, may also be used.

WAVE File names	f [kHz]	Angles		Measurement times		Rotation Direction	Setup
		Start heading	End heading	Start Time	End Time		
160232	2	31	33	160234	160645	Counter Clockwise	3
151755	2	134	31	151832	152228	Clockwise	2
100510	2	301	298	100510	100925	Clockwise	1
101024	2	298	302	101030	101433	Counter Clockwise	1
102050	3	302	301	102050	102453	Clockwise	1
102613	3	301	302	102624	103028	Counter Clockwise	1
95116	4	301	298	95132	95540	Clockwise	1
95315	4						
95515	4						
95710	4	298	301	95716	100116	Counter Clockwise	1
95910	4						
100110	4						

Table 4.2: Files used for directivity calculations and some additional information: frequency, angles of rotation, rotation direction and setup used.

### 4.4.1 Directivity diagram at 2 kHz

Figure 4.3 shows the clockwise and counter clockwise rotation data obtained from 2 WAVE files, with the Z and Y axis overlapped. It also shows the position of DAVS relative to the source, noting that when the rotation starts (0 degrees in polar plot axis) the DAVS Z axis was not exactly pointing to the source, but at approximately 15 degrees in the counter clockwise direction. Positive angles denote the clockwise rotation direction, while the counter clockwise directions is in the negative angles direction. Note also that there are some small discontinuity at start and end of the rotation due to bad alignment of acoustic data samples and heading data.

It can be noticed that at 2 kHz the "8" figure is well defined, for each axis. When the Y axis of the two accelerometers are parallel to the source their amplitude should be identical, as at 105°, however a small difference of accelerometer #50 at 75 degrees which was not expected to happen, can be noticed. When the Y axis is perpendicular to the source (15° and 165°) the expected attenuation occurs and the signal gets weaker between -8 and -16 dB, since the acoustic waves are perpendicular to the axis. With the Z axis at 15° and 165°, the waves cross accelerometer X axis parallel so the maximum intensity should occur, however due to the placement inside DAVS nose, a 2 to 3 dB difference between them can be noticed (see also C.2. The first accelerometer that the acoustic wave reaches has a lower amplitude value than the last reached. The rotation direction doesn't show any significant difference, being irrelevant which rotation direction is chosen.

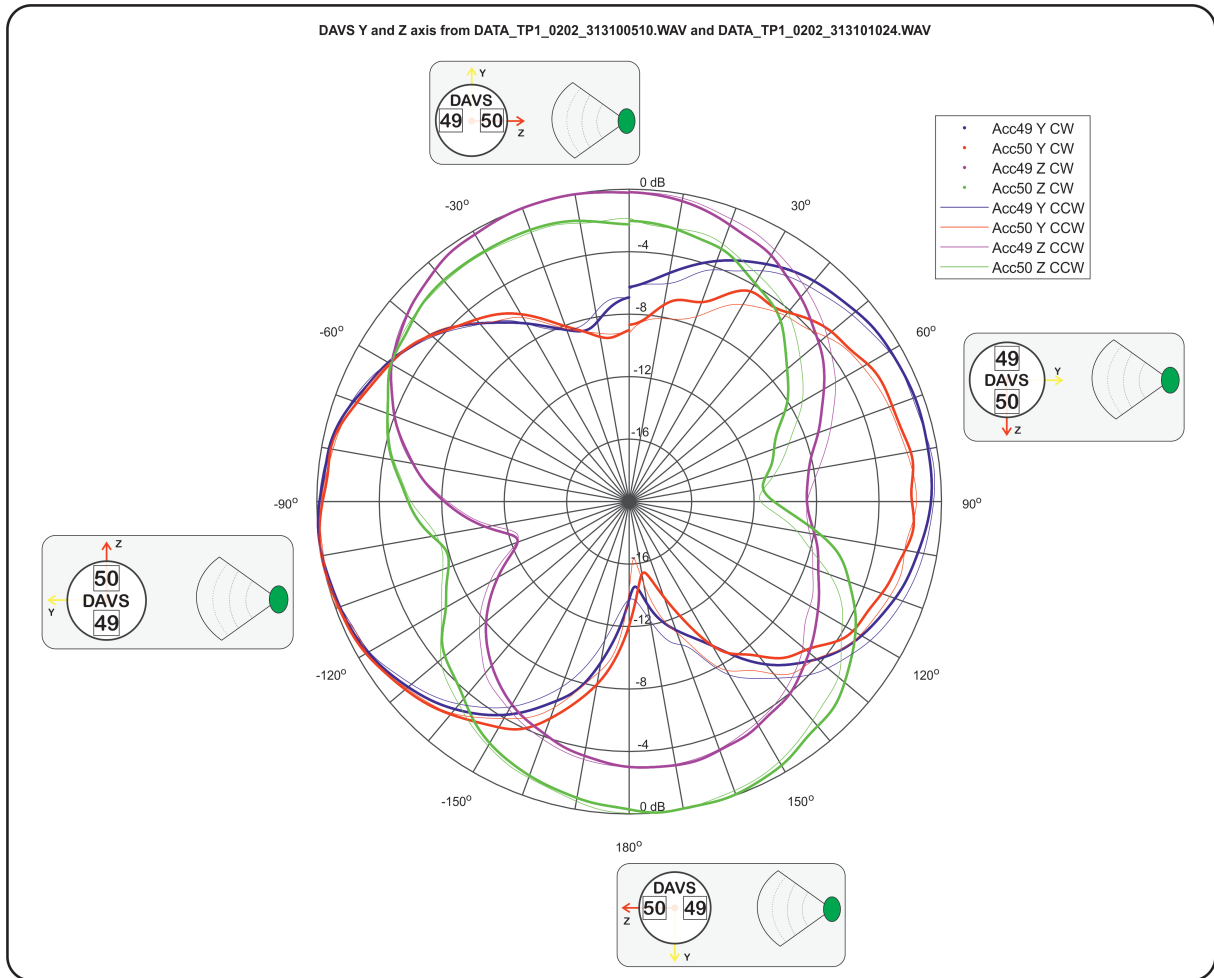


Figure 4.3: Directivity diagram at 2 kHz with CW and CCW rotation data plotted (Y-Z plane axis only).

#### 4.4.2 Directivity diagram at 3 kHz

The 3 kHz directivity diagram is shown in figure 4.4. A better pattern for Y axis rotation is obtained, were the two accelerometers follow identical values, while maintaining the expected "8" diagram pattern. However, for the Z axis a difference between accelerometers #49 and #50 still occurs, even if they swapped their values: at 2 kHz the weaker values were at accelerometer which first detects the acoustic wave, while at 3 kHz it has the strongest value. The "8" figure is also less visible, with a maximum attenuation around 10 dB (see C.5).

#### 4.4.3 Directivity diagram at 4 kHz

The directivity diagram obtained at 4 kHz is shown in figure 4.5. For this case the Y axis response follows the "8" figure for each accelerometer, as with the other frequencies (at 75° and -105°). However, for the Z axis the "8" figure almost disappeared. The first accelerometer crossed by the acoustic wave shows the normal gain, near 0 dB, while the accelerometer at the opposite side of DAVS nose present a large attenuation of approximately -8 dB (check C.8). This single lobe behaviour can be seen at angles -15°

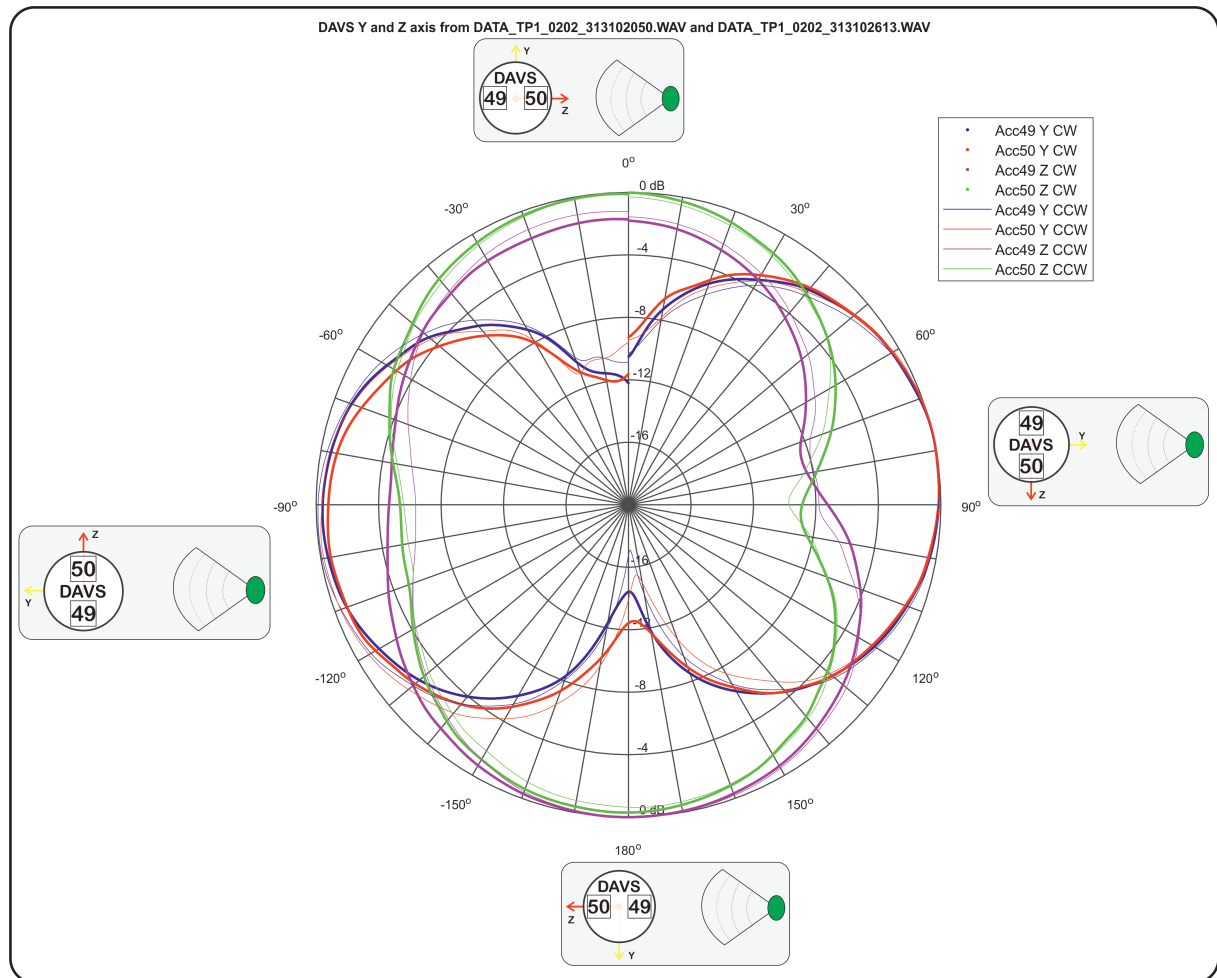


Figure 4.4: Directivity diagram at 3 kHz with CW and CCW rotation data plotted (Y-Z plane axis only).

for accelerometer #49 and at  $165^\circ$  for accelerometer #50. These behaviour was already seen on sensitivity calculations, where the accelerometer #49 present a significantly lower signal than accelerometer #50 (B.26).

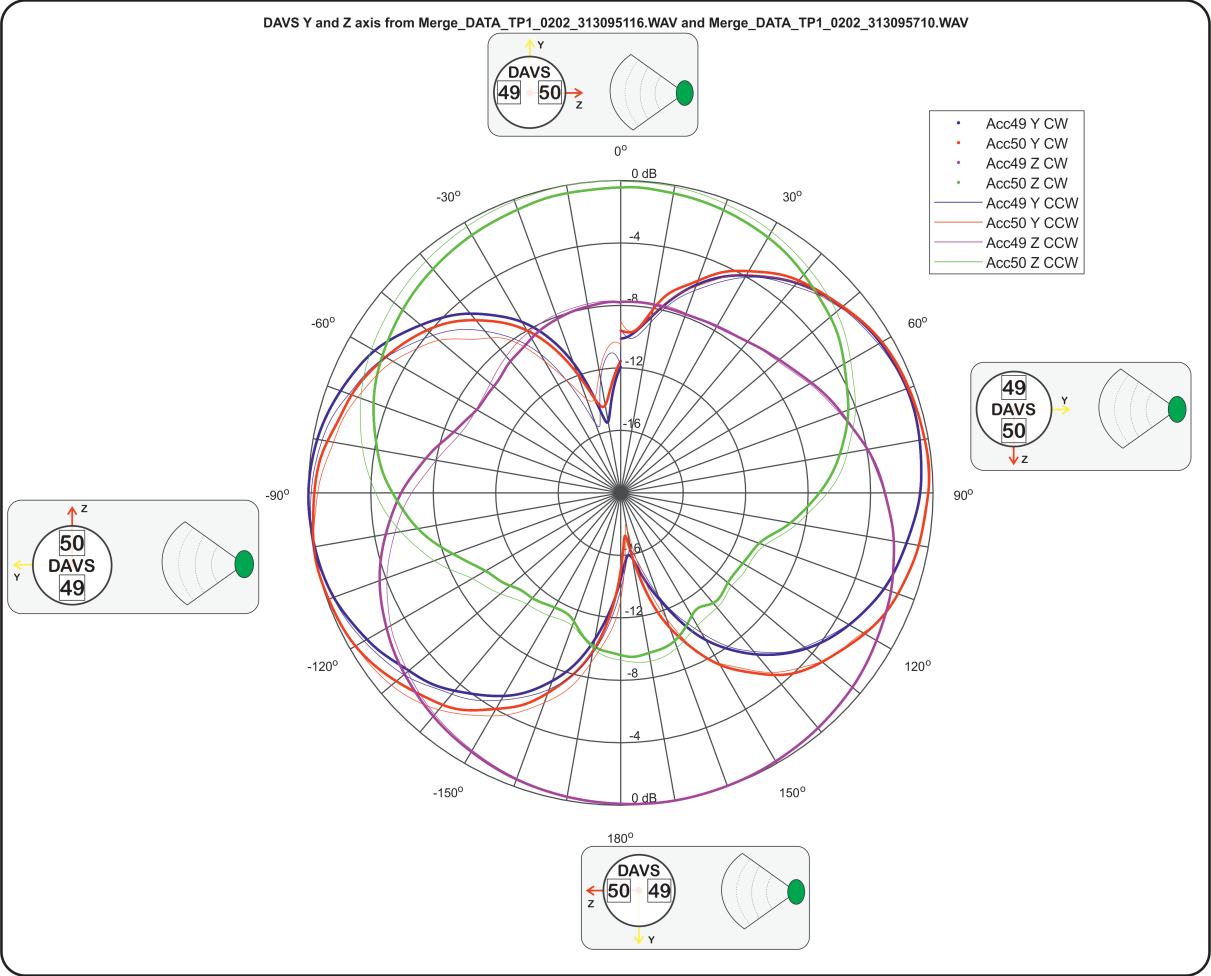


Figure 4.5: Directivity diagram at 4 kHz with CW and CCW rotation data plotted (Y-Z plane axis only).

# Chapter 5

## Results and Conclusions

From the analysis of the calibration testing data for sensitivity and directivity of DAVS sensor, the following conclusions may be drawn. The first and a general conclusion of this work is the importance of the review of the waveforms and the evaluation of their shapes. This will allow for the identification of significant interference that may exist on the captures.

Then, while evaluating the hydrophone sensitivity, and when comparing the results achieved by this work with those of report [1] there are some slight differences. These differences came essentially from the analysis methodology. When Y axis is pointing to the source, the maximum difference between the two reports is 1.5 dB with all obtained values into  $-195 \pm 3$  dB. The obtained values when the Z axis is pointing to the source are very close to the ones from Y axis, as expected for an omnidirectional device (except for 2 kHz case, due to a bad measurement). When looking at the waveform, the lower frequencies of 1 and 0.5 kHz shows the existence of interference that significantly distort the signal. This was the expected behaviour due to tank size limitations.

The accelerometer sensitivity results are more difficult to analyze. For the Y axis experiment, the two accelerometers showed that they have similar values, as expected, due to their physical placement on DAVS. This experiment placed the two accelerometers aligned in a position where the wave front reaches them at the same time. However, when the Z axis is pointing to the source, the accelerometer position is rotated 90 degrees and there is one in front of the other, causing some mutual interference. This can be seen at the 2, 3 and 4 kHz responses, where each accelerometer shows a very distinct value. The experiment has been done in a position where the wave front reaches accelerometer 50 before 49. A similar experiment must be done inverting accelerometer positions, to confirm the response variation that happened in this case. When looking at the 3 axis waveforms of each accelerometer a strong cross talk can be seen across the experiment. For the Y-Z plane, cross talk can be caused by any lateral reflections from the tank, but it is not very clear. Some testing on open waters, where no lateral reflections exist must be done to check this. The support structure, transducer placement into sensing element (inside DAVS nose) and DAVS body can also cause some reflections or resonance, which translate into the unwanted detected lateral components. More testing is required to conclude about it.

The directionality tests show that there is some distinct behaviour depending on the position of accelerometers relative to the source. When they are both perpendicular to the source (Y axis facing the front wave), the axis response has an eight pattern with the 2 main lobes facing the source for all frequencies, as expected and as happened with

sensitivity. When accelerometers are colinear with the source (Z axis facing wave front), the response depends on the relative position of accelerometers inside DAVS nose and change for each frequency.

The experiments done allowed us to obtain some data about DAVS responses. However, there are some identified errors in the measurement data, which we must be aware when analysing these results. The lack of redundant data, did not allowed to double check the results. This is something that should be taken into account for future experiments.

The attachment setup should also be chosen and maintained during experiments, since the used support structures will influence the measurements. We should use some structure that leaves DAVS suspended and not directly attached to a rigid structure, but we don't have that type of structure. So we should consider some error introduced by fixation method, that we can not quantify. Doing the same tests, with the same setup but changing the support structure will be an interesting experiment to evaluate how it affect the measurements.

Another interesting experiment for the future is the use of more tone frequencies, to cover intermediate zones and expand the tested range to higher frequencies. This will allow us to increase the sensitivity resolution and see how DAVS performs between the frequencies used in this work. If for the hydrophone the variations will not be significant, the accelerometer results show that big differences could happen, as the ones from 1 kHz to 2 kHz in this experiments.

# Bibliography

- [1] A. Mantouka, P. Felisberto, P. Santos, and F. Zabel. Calibration of dual accelerometer vector sensor at the arsenal tank. Siplab technical report 04/17, April 2017.
- [2] WiMUST project. Widely scalable mobile underwater sonar technology. <http://www.wimust.eu/>, Last accessed on 2020-05-20.
- [3] A. Mantouka, P. Felisberto, c. Soares, F. Zabel, and S. M. Jesus. Wimust'17 sines trial: Seismic data report. Siplab technical report 07/17, December 2017.
- [4] N. Pinto and S. M. Jesus. Calibration methods for vector sensors. Siplab technical report 03/20, July 2020.
- [5] N. Pinto and S. M. Jesus. Dual accelerometer vector sensor - user manual. Siplab technical report 02/20, March 2020.
- [6] John L. Butler and Charles H. Sherman. *Transducers and arrays for underwater sound*. Springer, 2016.
- [7] Robert J. Bobber. *Underwater electroacoustic measurements*. Naval Research Laboratory, 1970.
- [8] Peter Levin. Calibration of hydrophones. Technical Report 1-1973, Bruel and Kjaer, 1973.
- [9] X. Lurton. *Underwater Acoustics: An Introduction*. Springer Praxis Books. Springer Berlin Heidelberg, 2011.

# Appendices

## A DAVS additional formulas

### A.1 Hydrophone Sensitivity

The sensitivity of a hydrophone  $S_{hyd}$  (also called receiving voltage sensitivity, RVS [6] or free field voltage sensitivity [7, 8]) can be written in terms of the relation between the open circuit voltage (OCV/OCRR) at hydrophone terminals  $V_{hyd}$  and the incident free field pressure  $P_{hyd}$  of a plane wave, in  $\mu$ Pascal units as

$$S_{hyd} = \frac{V_{hyd}}{P_{hyd}} \left[ \frac{V}{\mu Pa} \right]. \quad (1)$$

This sensitivity is frequency dependent, even if usually it's expressed without consider the frequency variation, for a so called flat range, a band of frequencies where the variation is lower than some value (like 3dB).

Sensitivity is also commonly expressed in decibel units, as the electrical voltage for an incident pressure of 1  $\mu Pa$  and a reference voltage of 1 Volt (sensitivity relative to  $(1V)/(1\mu Pa)$ ) [9] as

$$S_{hyd} \left[ \text{dB re } \frac{V}{\mu Pa} \right] = 20 * \log \left( \frac{V_{hyd}}{P_{hyd}} \left[ \frac{V}{\mu Pa} \right] \right). \quad (2)$$

## B DAVS Sensitivity Waveforms

The following subchapters (from B.1 to B.9) contains three images each that shows the DAVS hydrophone, accelerometer and the reference Reson voltage waveforms, obtained from the first pulse of WAVE files. The first image compares the DAVS hydrophone voltage with Reson voltage, and have the 20 peaks identified. The red line represent the mean values of the selected peaks and the green line is the RMS voltage value used for sensitivity calculations. 2 vertical dashed lines represent the range of peaks used for the mean calculations. The second image shows the Y or Z axis voltage waveforms from the two accelerometers overlapped. The RMS voltage values are represented by the red (accelerometer 49) and blue (accelerometer 50) trace. 2 vertical dashed lines represent the range of peaks used for the mean calculations. The third image shows each accelerometer three axis waveforms of the selected pulse to check cross talk between axis. The left side figure have the waveforms for accelerometer 49 while right side shows the accelerometer 50 waveforms. The last 4 chapters show in one figure some graph of subchapters B.1 to B.9, allowing an easy comparison between them.

### B.1 Y Axis Sensitivity at 1 kHz

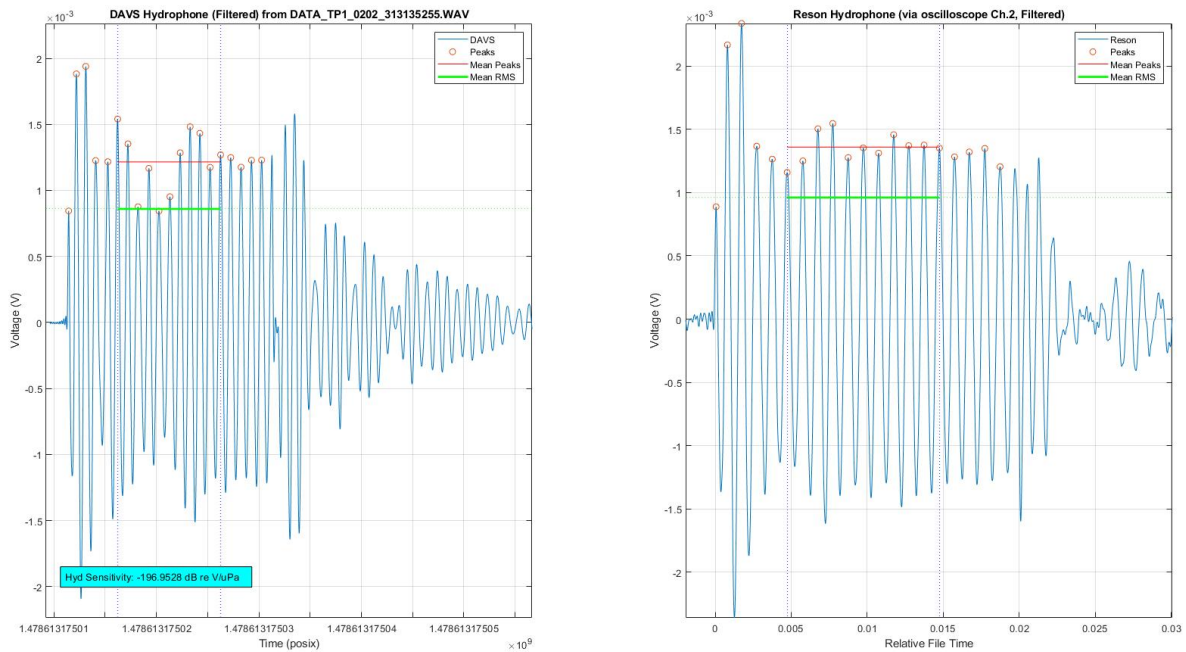


Figure B.1: DAVS hydrophone and reference hydrophone waveforms and RMS values for Y axis 1 kHz (Reson hydrophone near source)

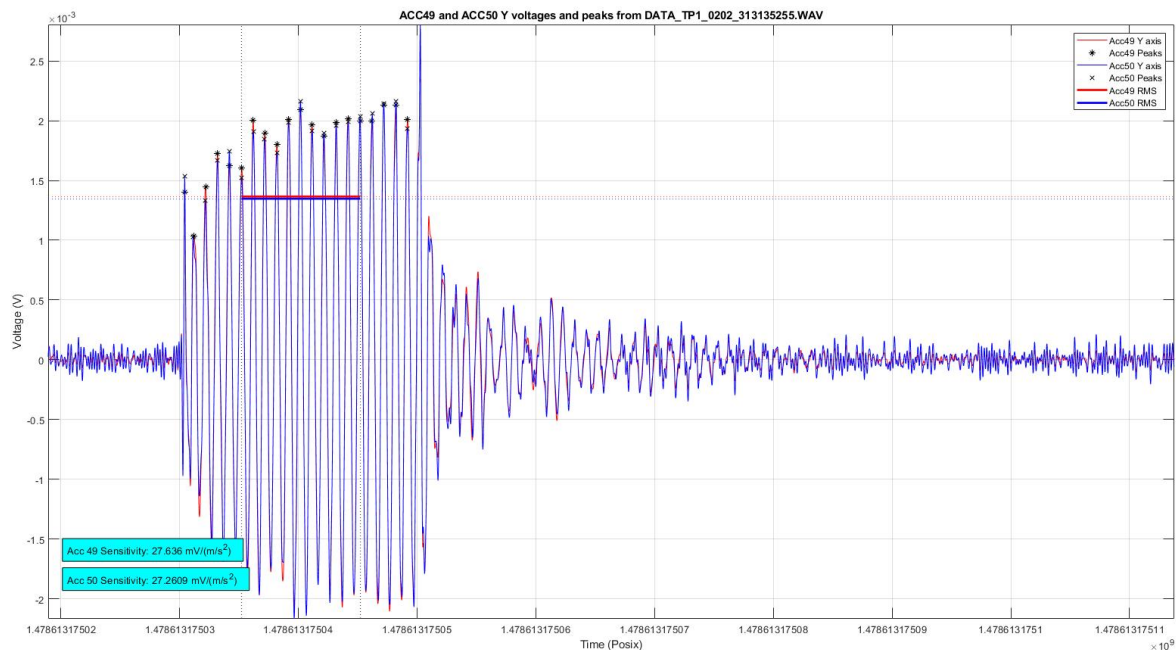


Figure B.2: Accelerometer waveforms and RMS values for Y axis 1 kHz

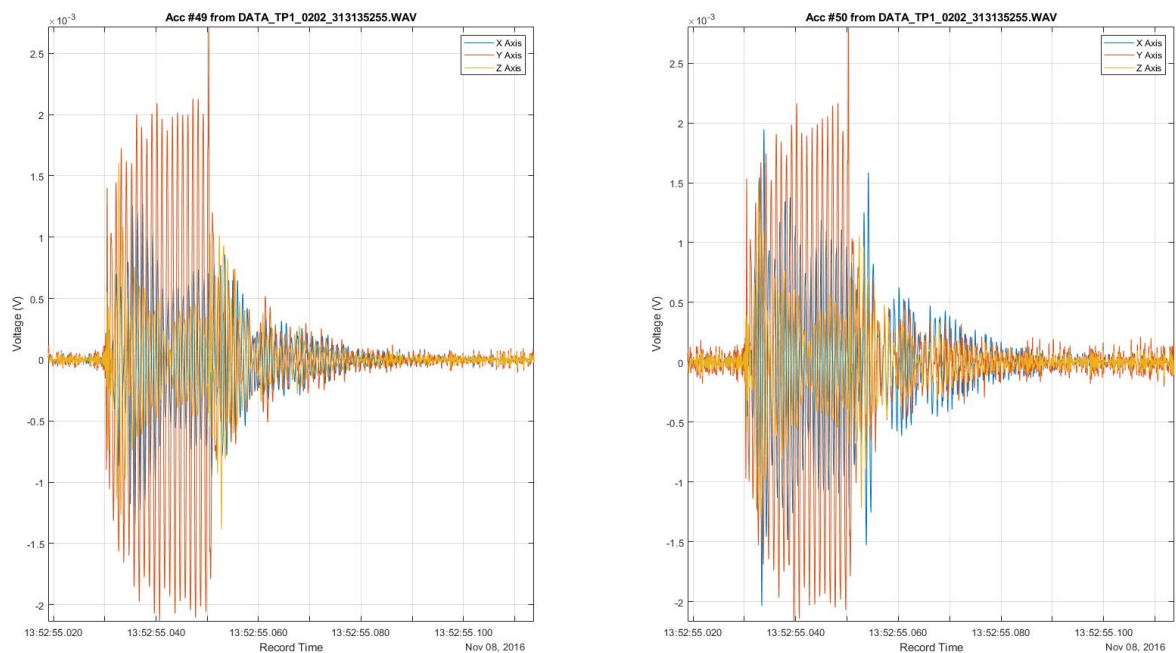


Figure B.3: Accelerometer waveforms for all axis at 1 kHz

## B.2 Y Axis Sensitivity at 2 kHz

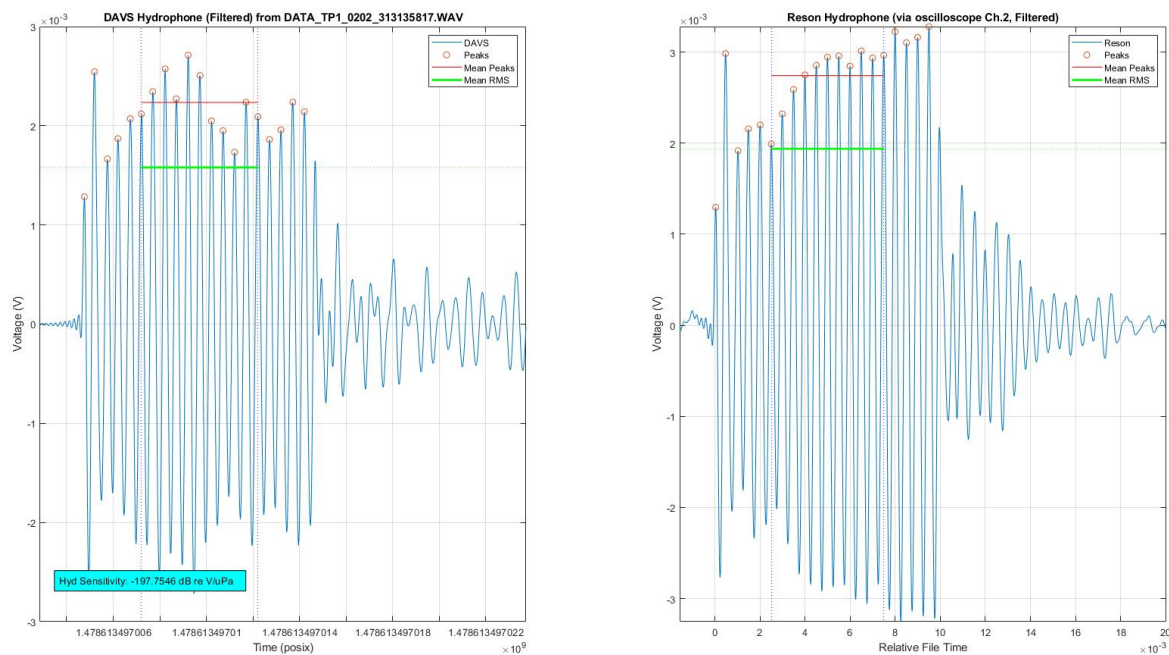


Figure B.4: DAVS hydrophone and reference hydrophone waveforms and RMS values for Y axis 2 kHz (Reson hydrophone near source)

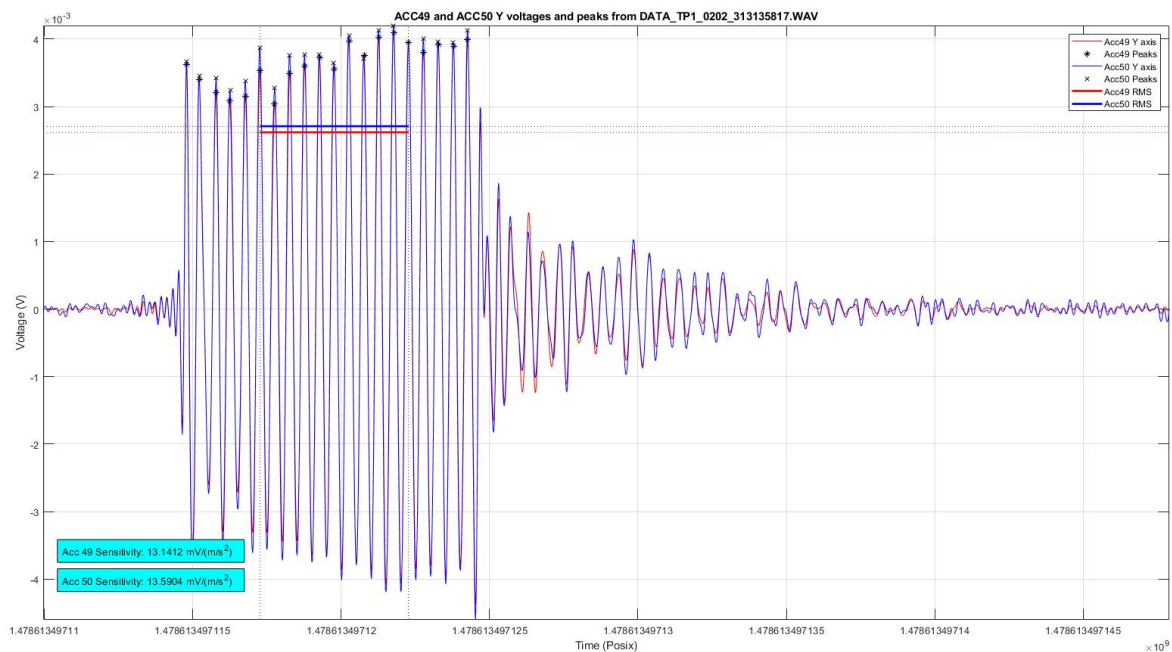


Figure B.5: Accelerometer waveforms and RMS values for Y axis 2 kHz

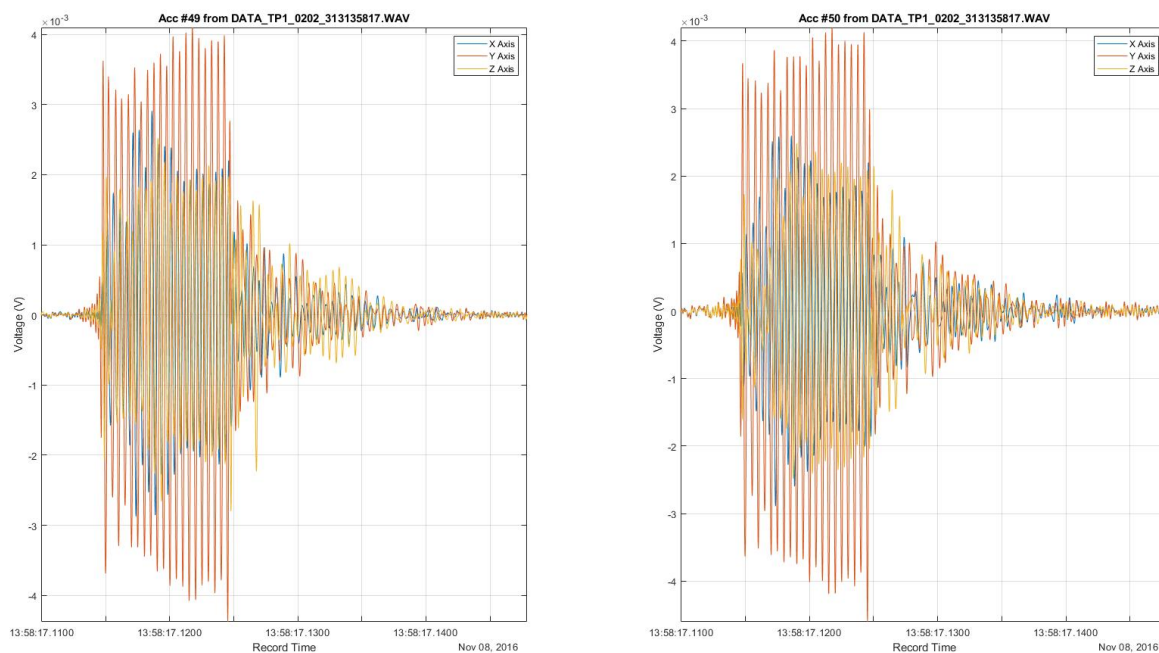


Figure B.6: Accelerometer waveforms for all axis at 2 kHz

### B.3 Y Axis Sensitivity at 3 kHz

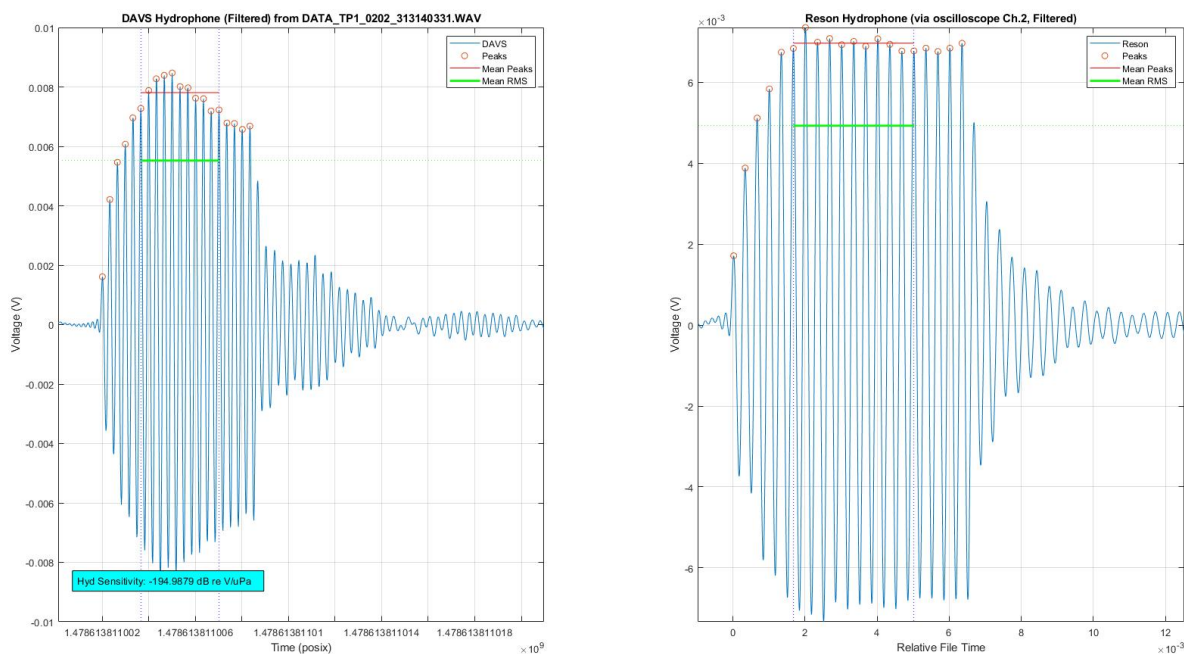


Figure B.7: DAVS hydrophone and reference hydrophone waveforms and RMS values for Y axis 3 kHz (Reson hydrophone near source)

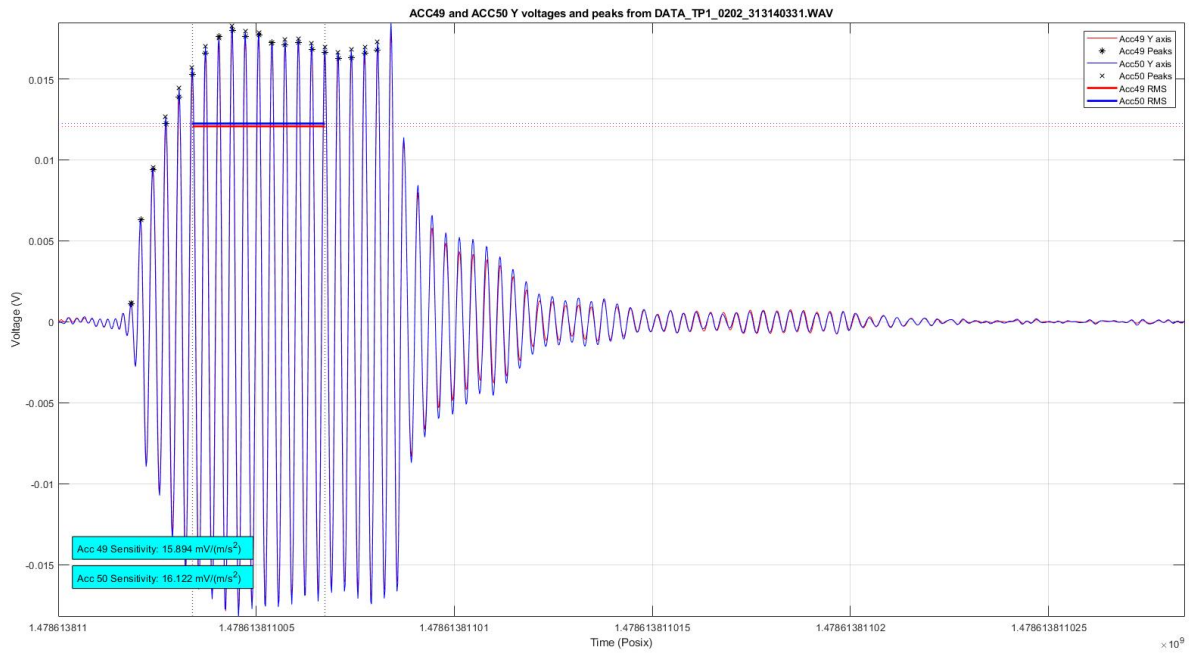


Figure B.8: Accelerometer waveforms and RMS values for Y axis 3 kHz

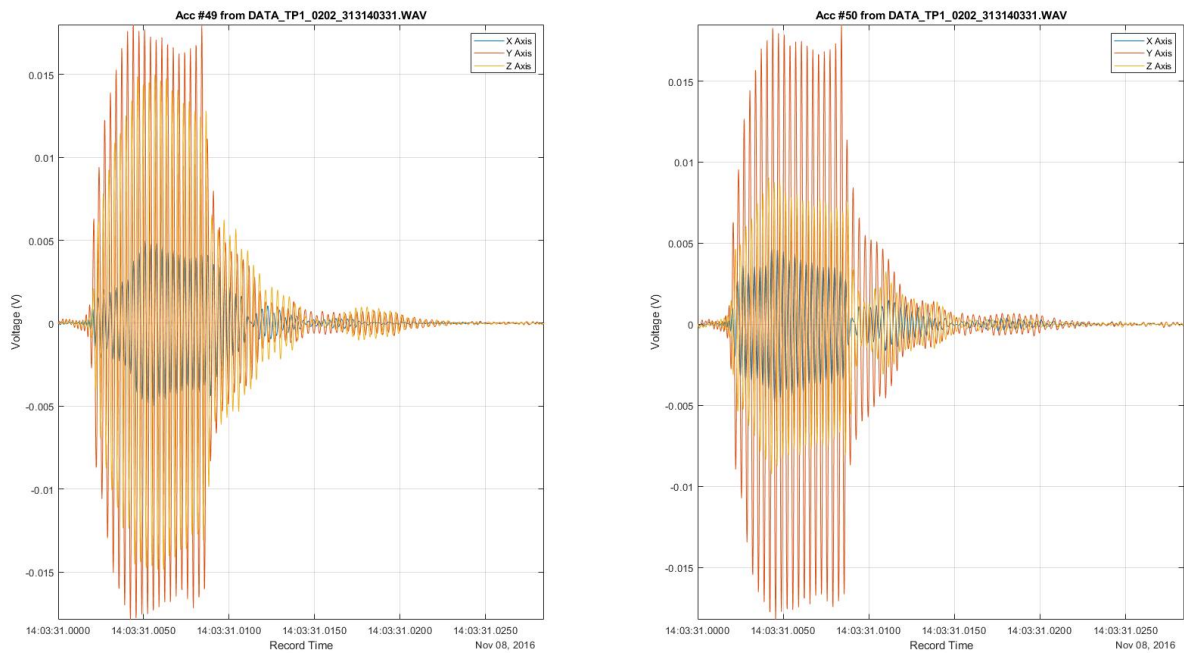


Figure B.9: Accelerometer waveforms for all axis at 3 kHz

### B.4 Y Axis Sensitivity at 4 kHz

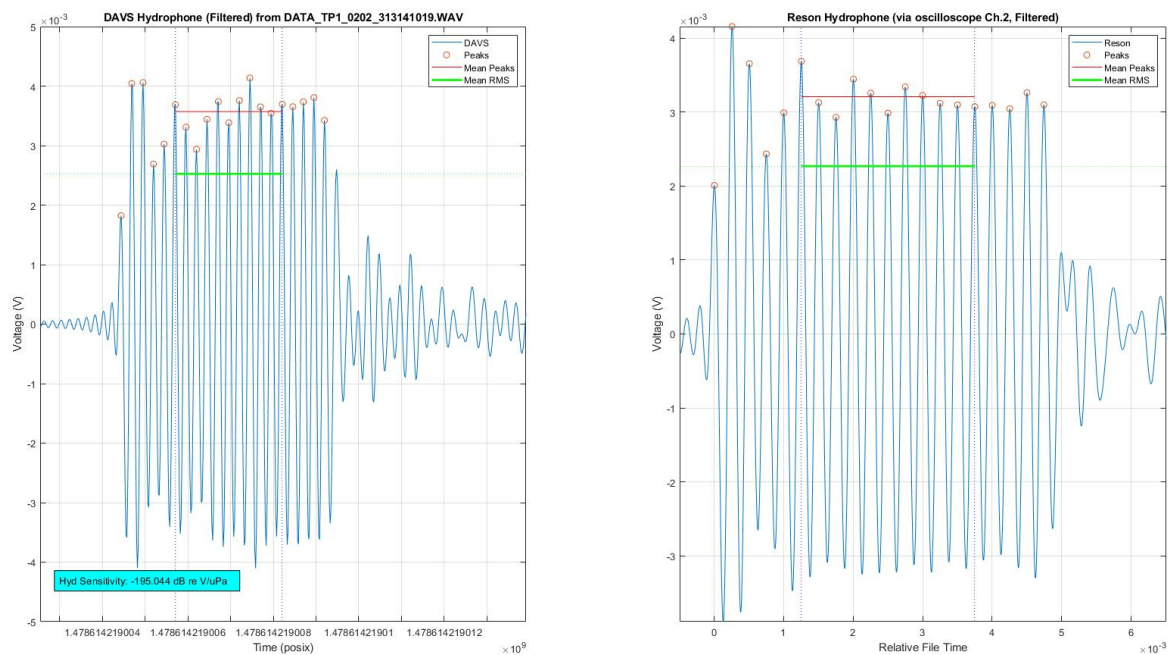


Figure B.10: DAVS hydrophone and reference hydrophone waveforms and RMS values for Y axis 4 kHz (Reson hydrophone near source)

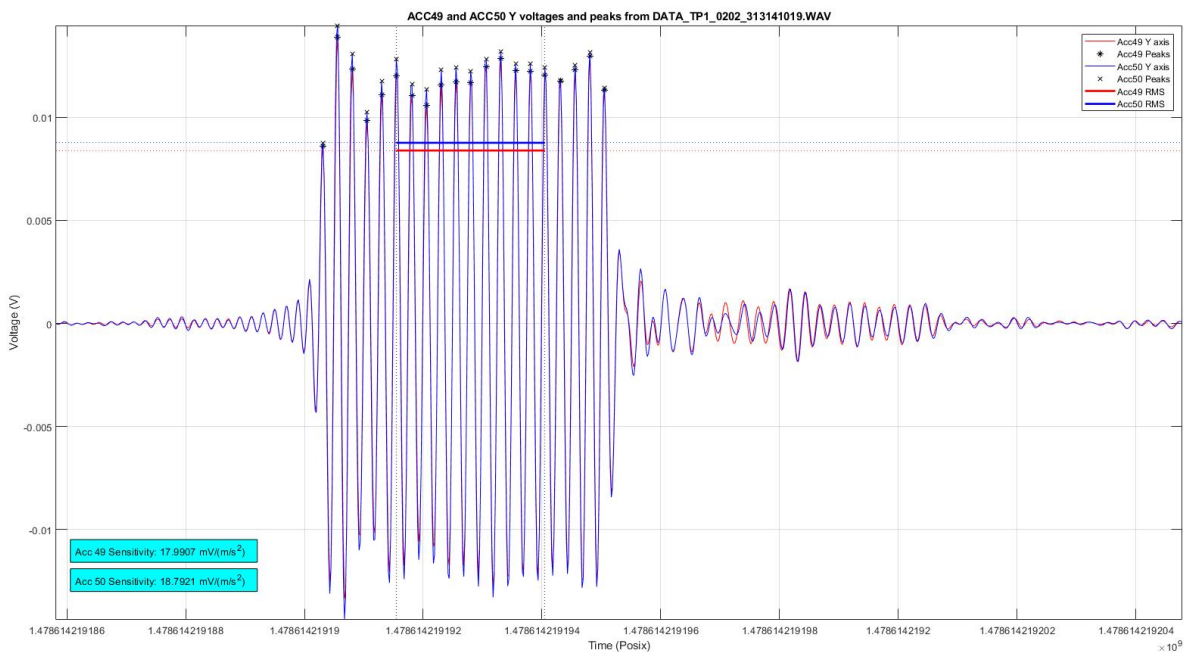


Figure B.11: Accelerometer waveforms and RMS values for Y axis 4 kHz

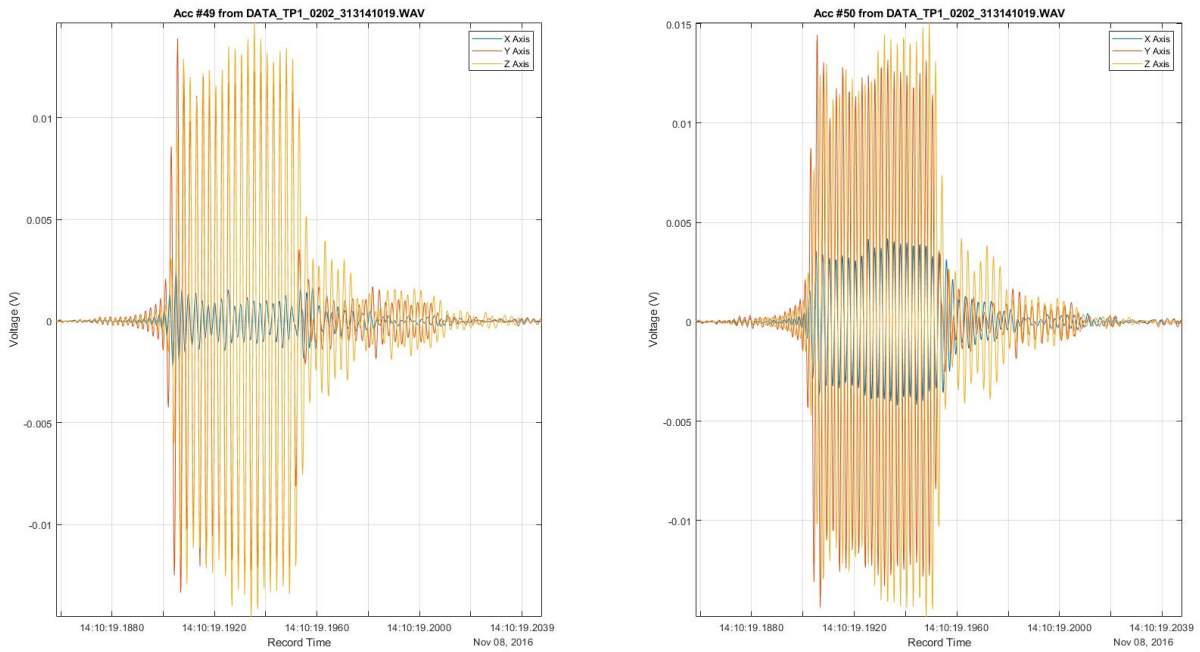


Figure B.12: Accelerometer waveforms for all axis at 4 kHz

### B.5 Z Axis Sensitivity at 0.5 kHz

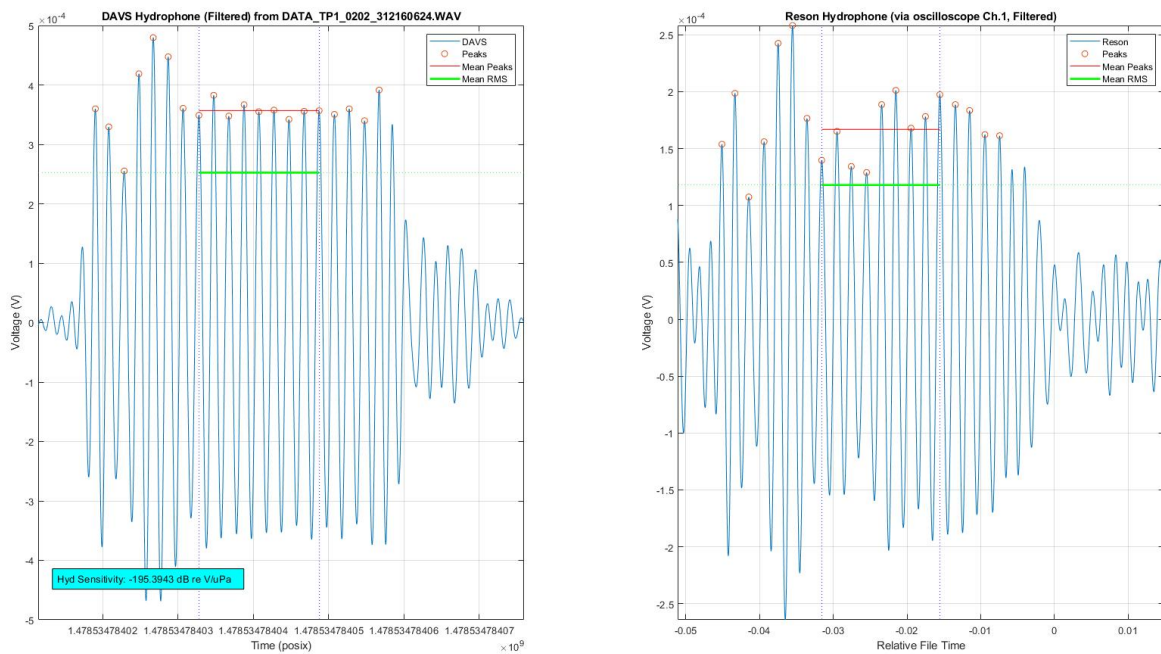


Figure B.13: DAVS hydrophone and reference hydrophone waveforms and RMS values for Z axis 0.5 kHz

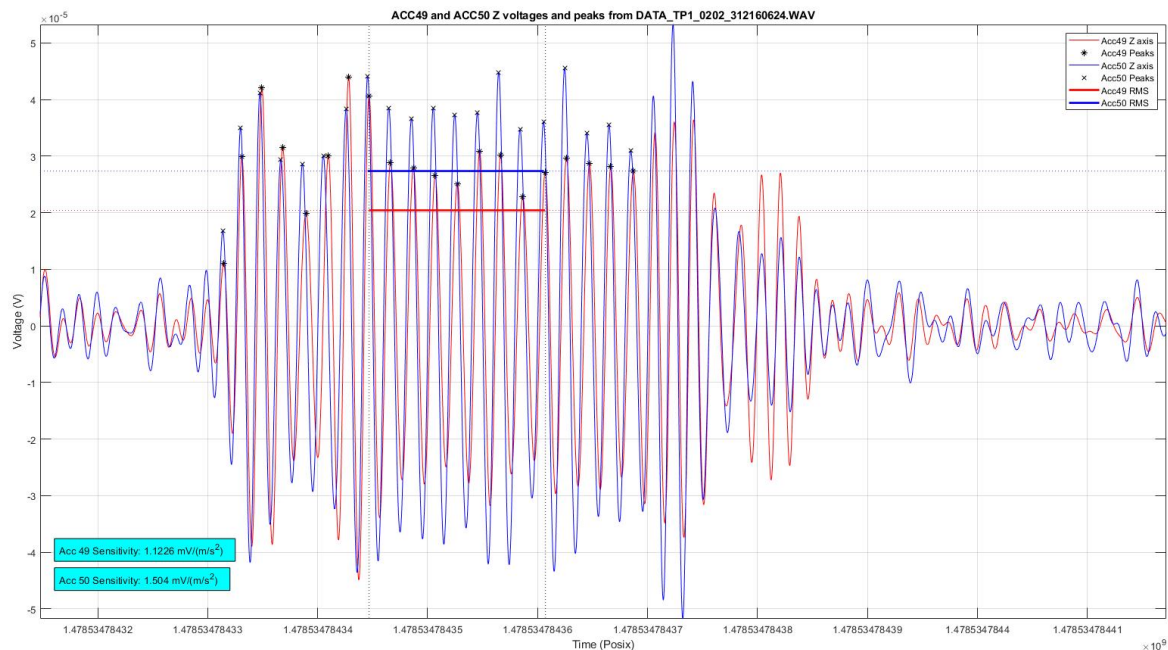


Figure B.14: Accelerometer waveforms and RMS values for Z axis 0.5 kHz

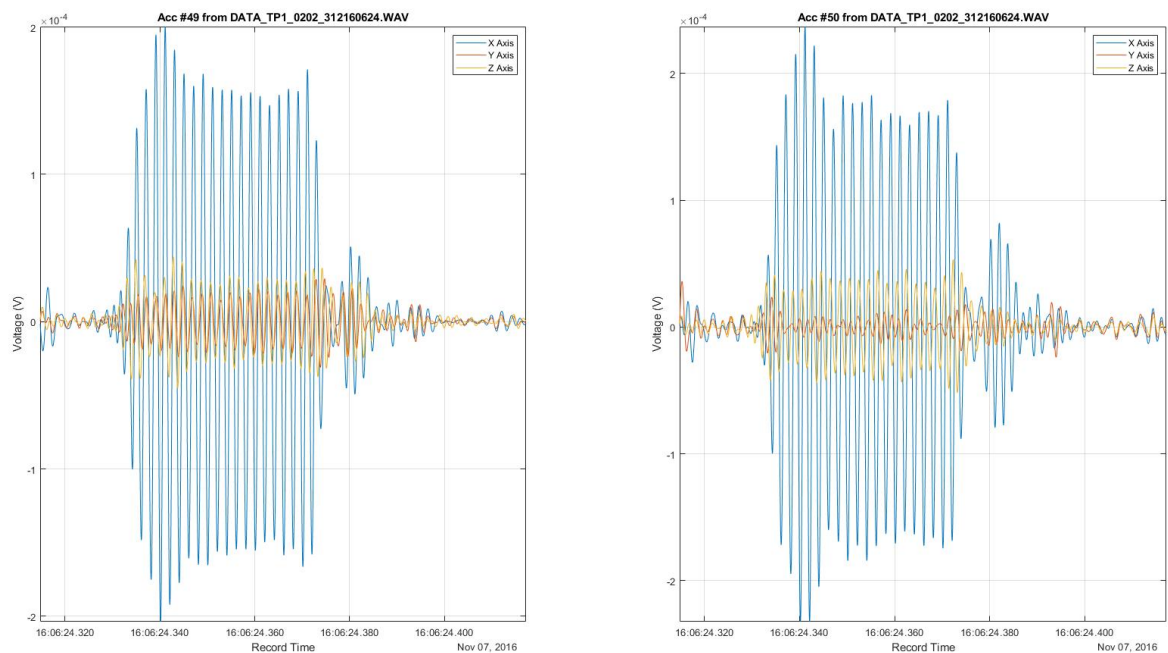


Figure B.15: Accelerometer waveforms for all axis at 0.5 kHz

## B.6 Z Axis Sensitivity at 1 kHz

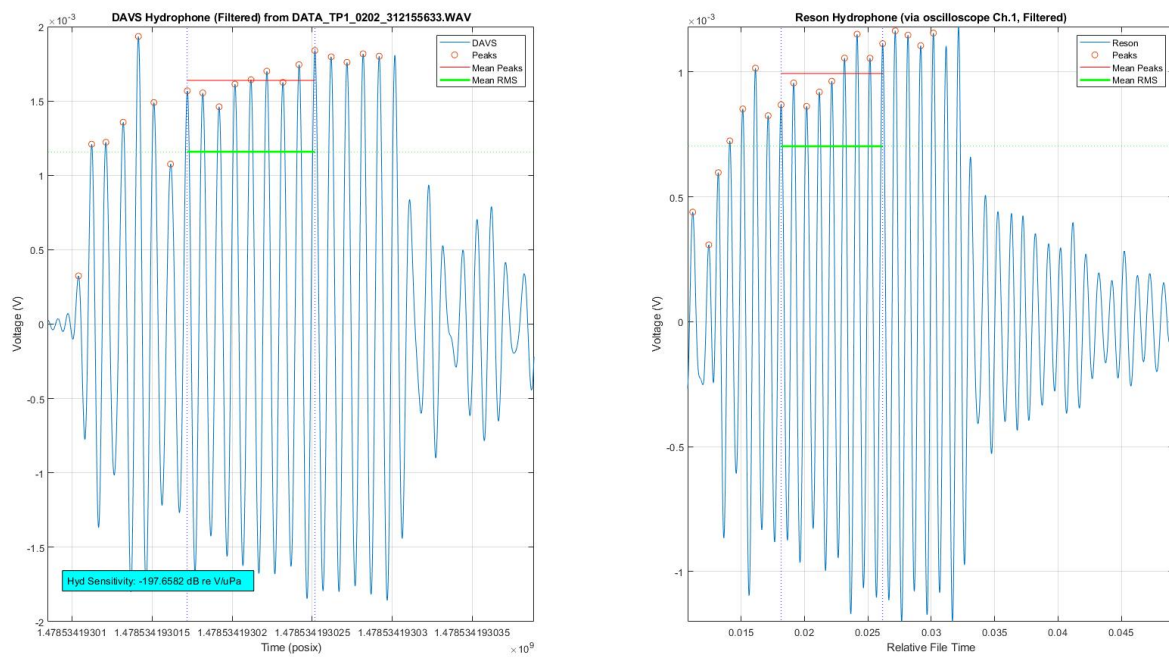


Figure B.16: DAVS hydrophone and reference hydrophone waveforms and RMS values for Z axis 1 kHz

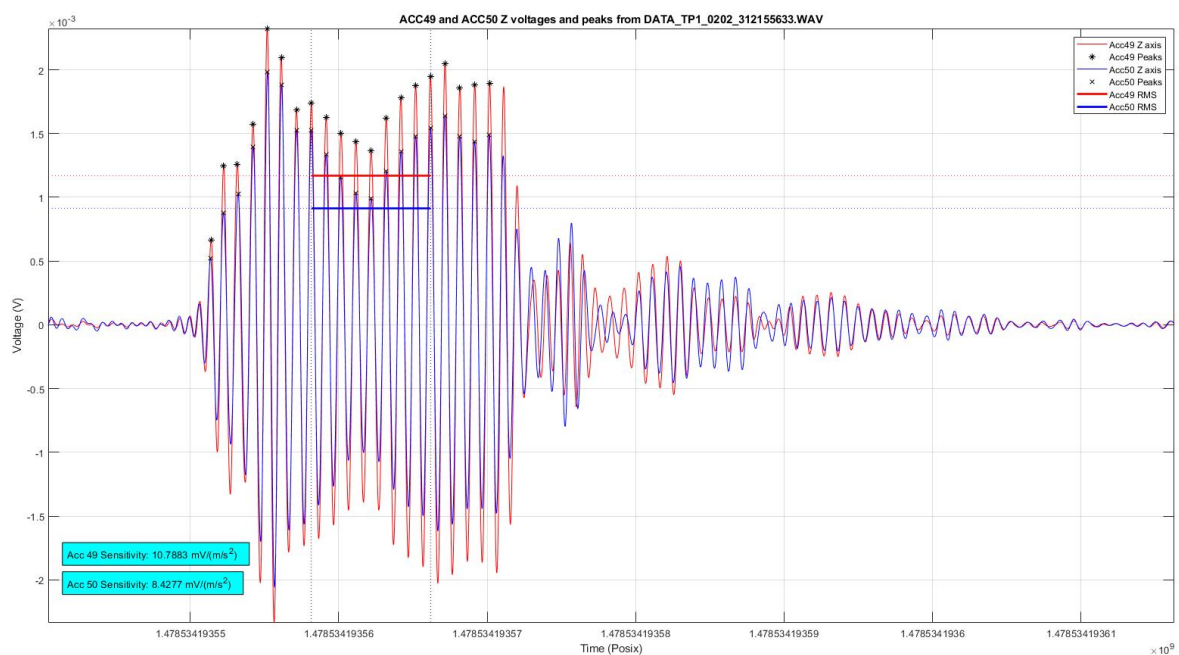


Figure B.17: Accelerometer waveforms and RMS values for Z axis 1 kHz

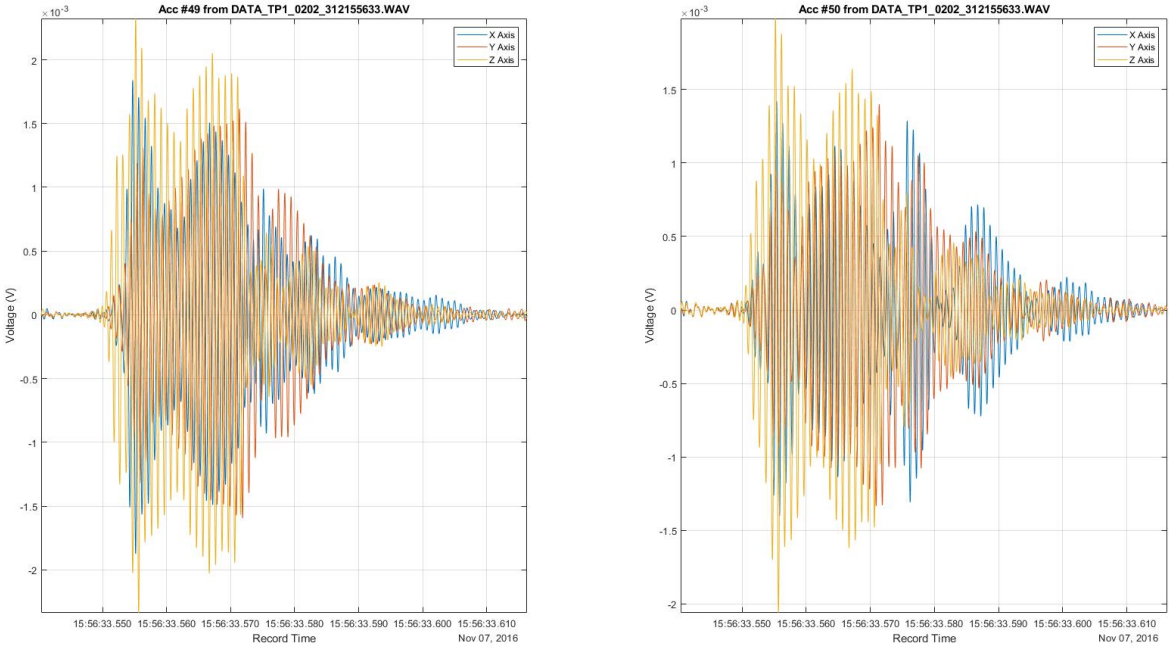


Figure B.18: Accelerometer waveforms for all axis at 1 kHz

### B.7 Z Axis Sensitivity at 2 kHz

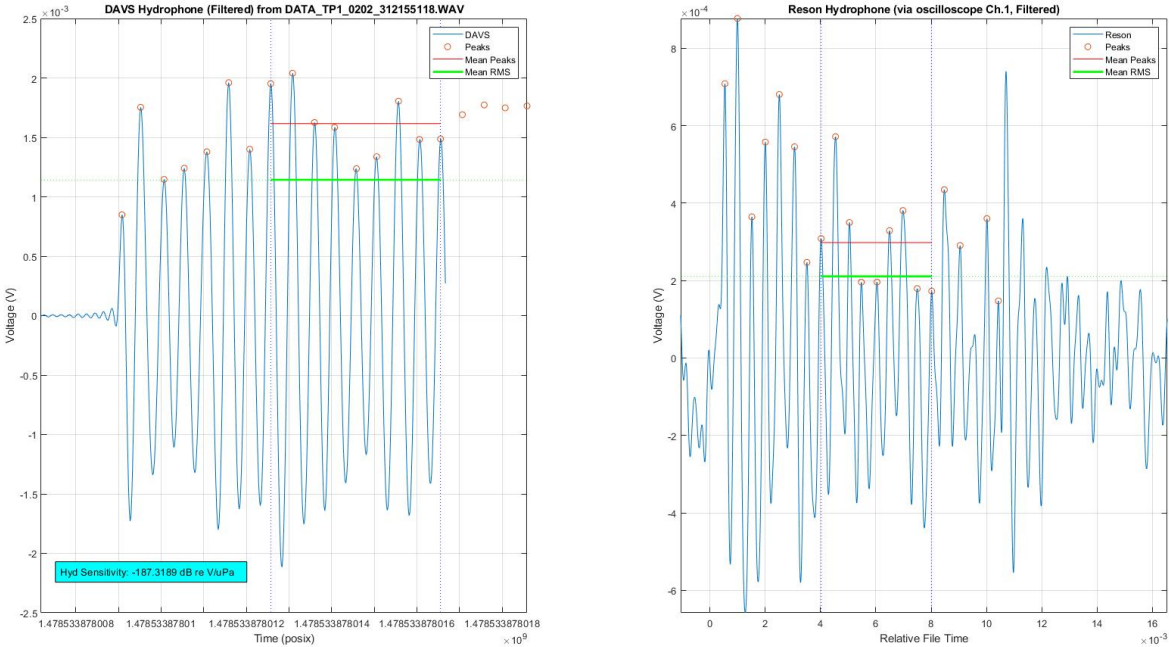


Figure B.19: DAVS hydrophone and reference hydrophone waveforms and RMS values for Z axis 2 kHz

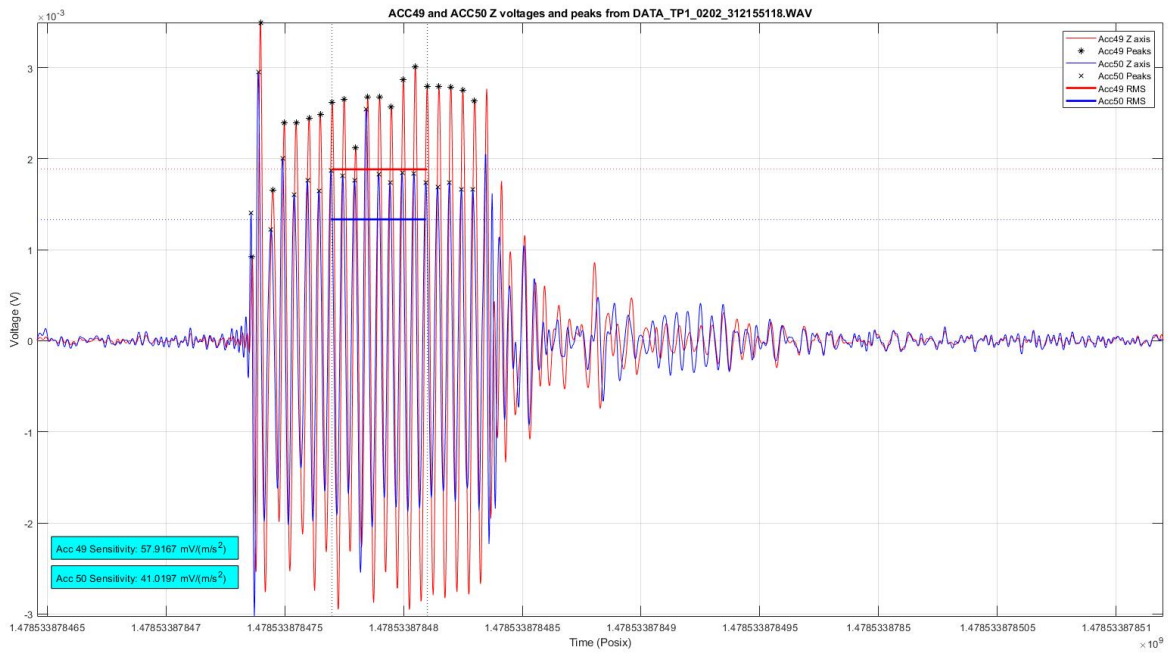


Figure B.20: Accelerometer waveforms and RMS values for Z axis 2 kHz

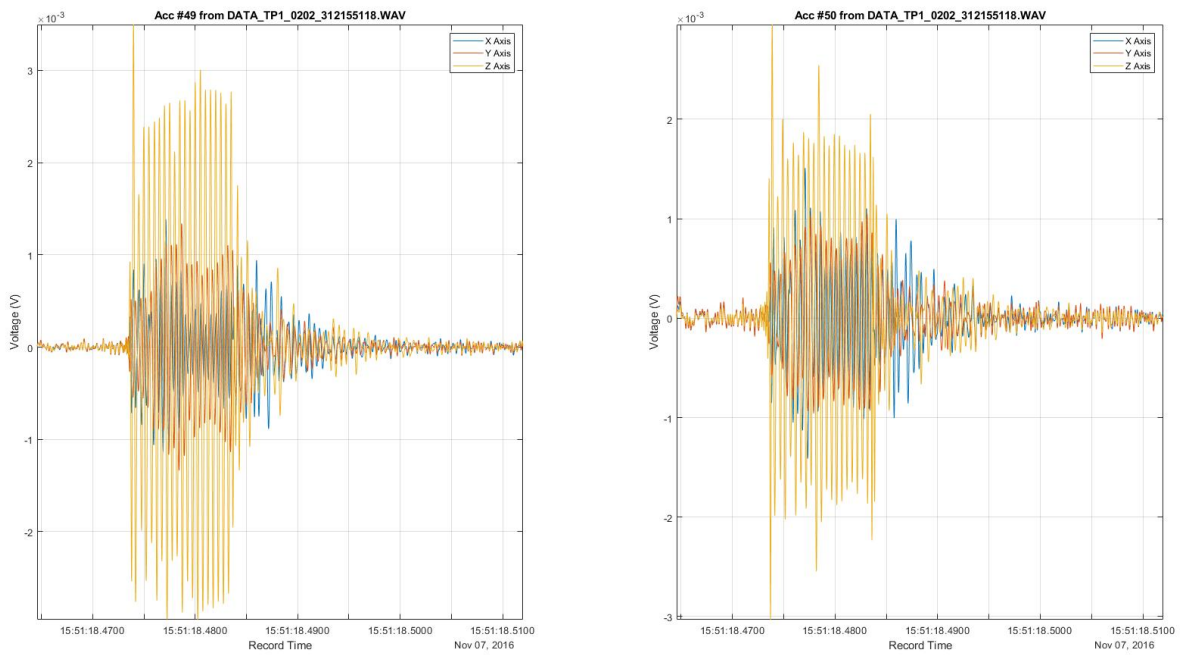


Figure B.21: Accelerometer waveforms for all axis at 2 kHz

### B.8 Z Axis Sensitivity at 3 kHz

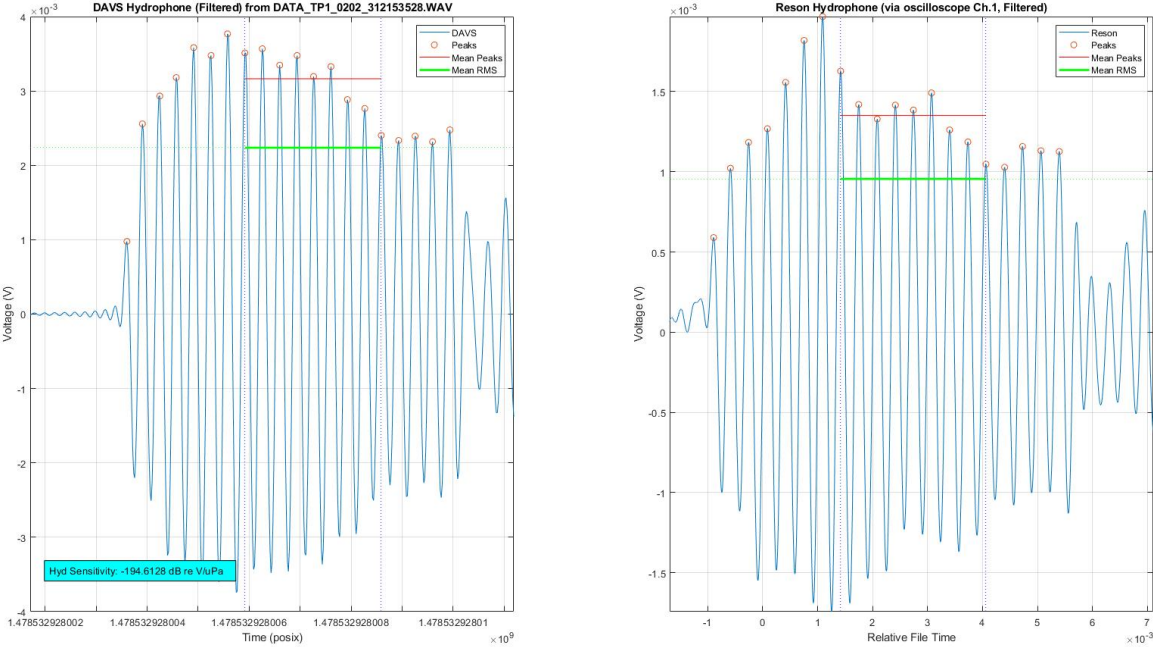


Figure B.22: DAVS hydrophone and reference hydrophone waveforms and RMS values for Z axis 3 kHz

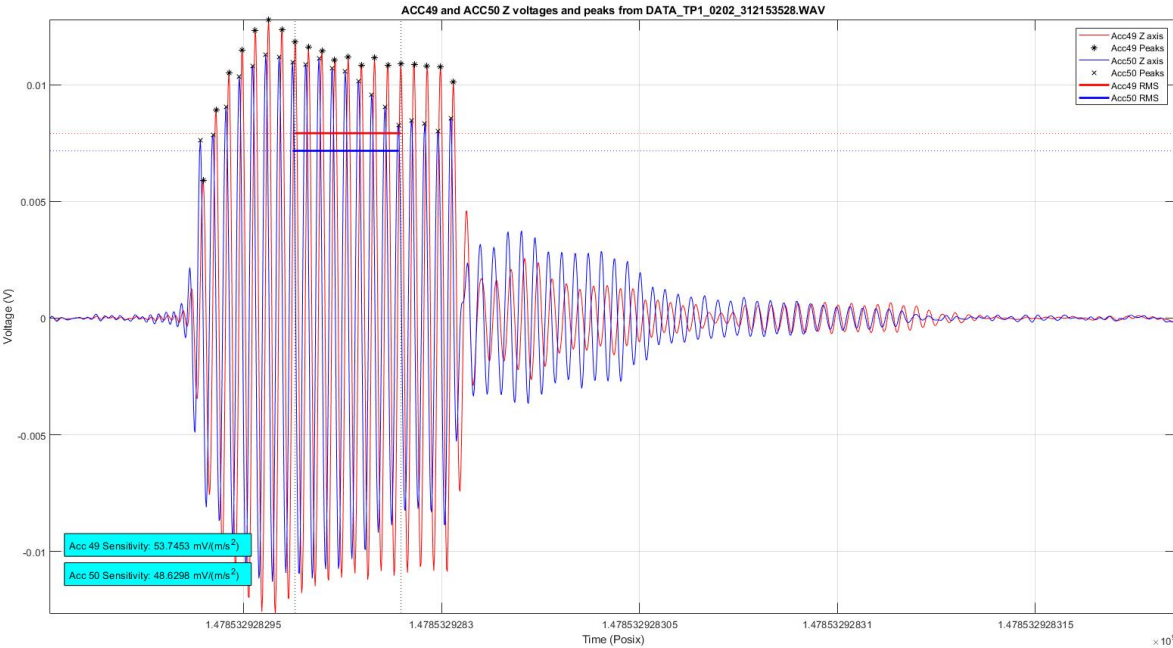


Figure B.23: Accelerometer waveforms and RMS values for Z axis 3 kHz

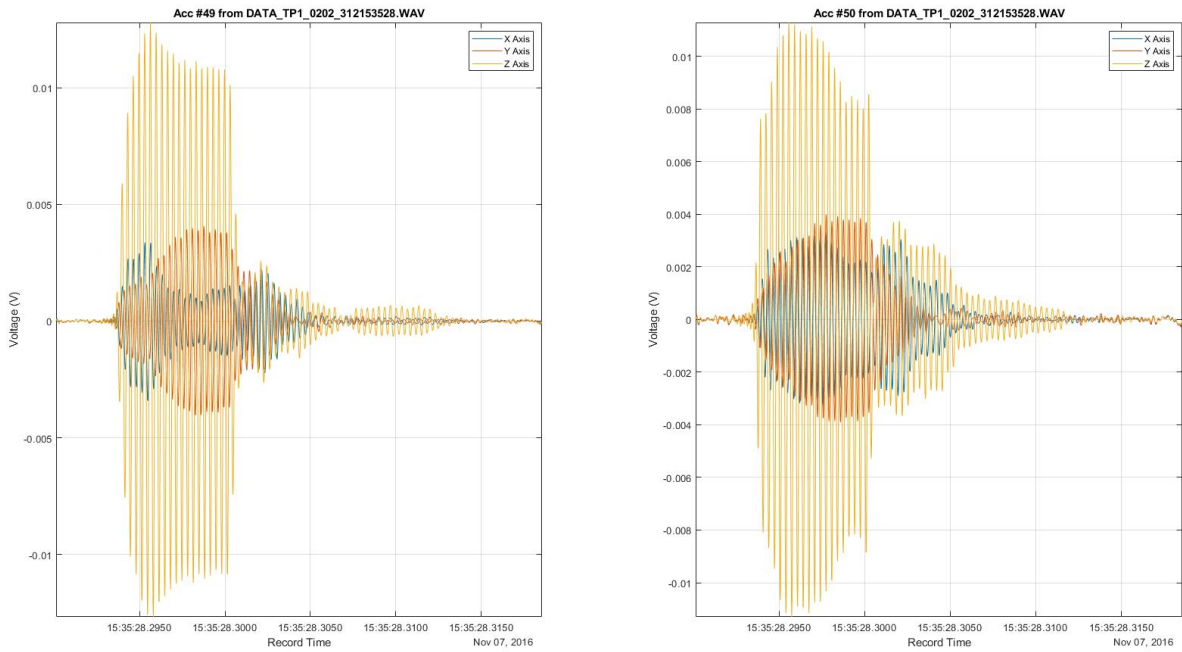


Figure B.24: Accelerometer waveforms for all axis at 3 kHz

### B.9 Z Axis Sensitivity at 4 kHz

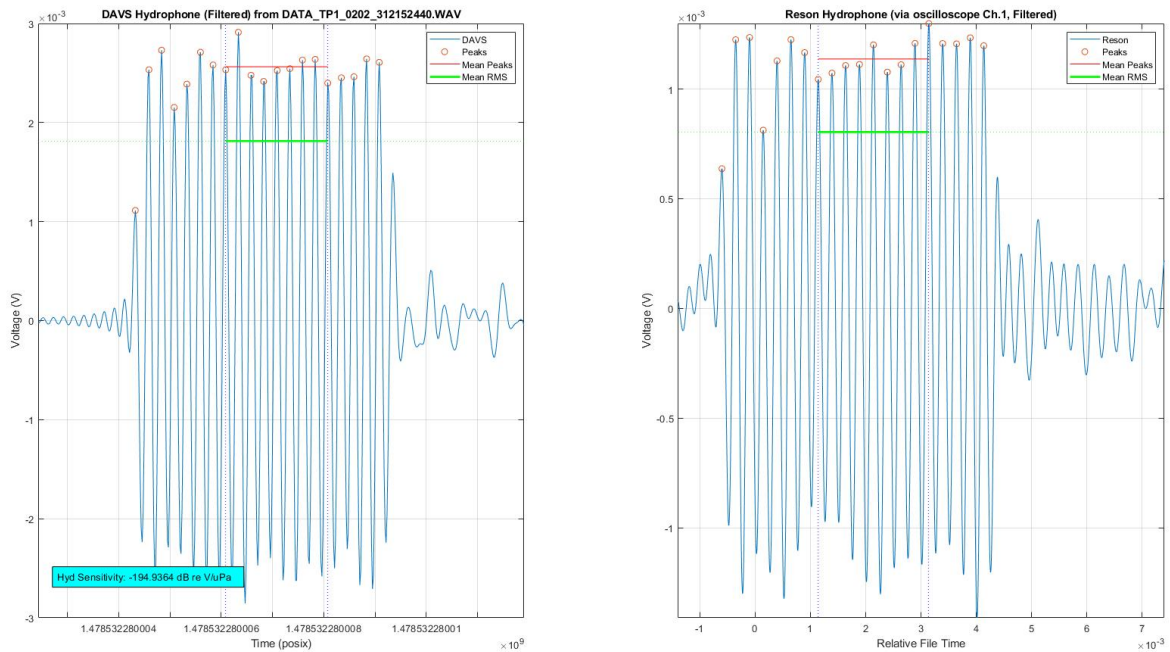


Figure B.25: DAVS hydrophone and reference hydrophone waveforms and RMS values for Z axis 4 kHz

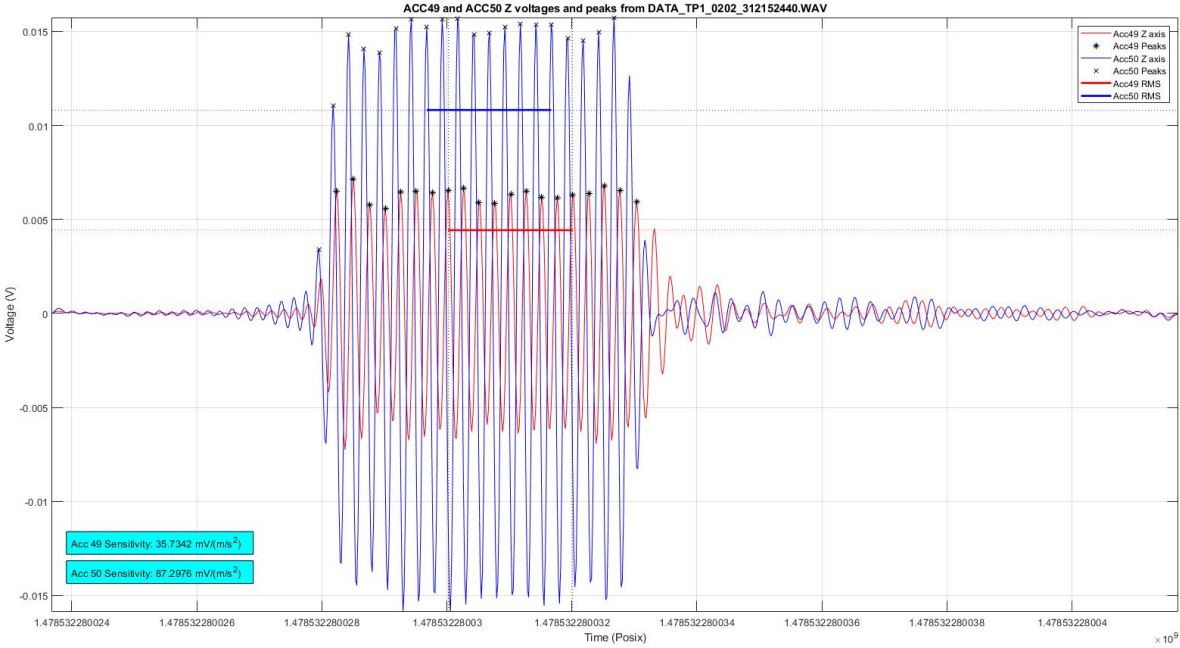


Figure B.26: Accelerometer waveforms and RMS values for Z axis 4 kHz

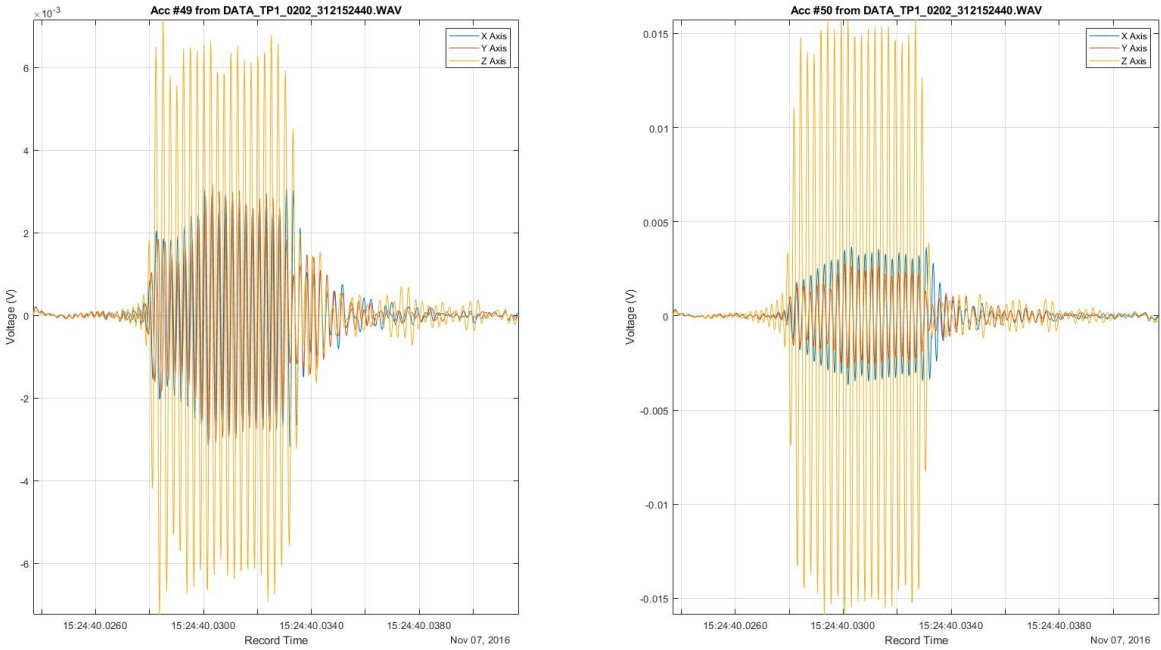
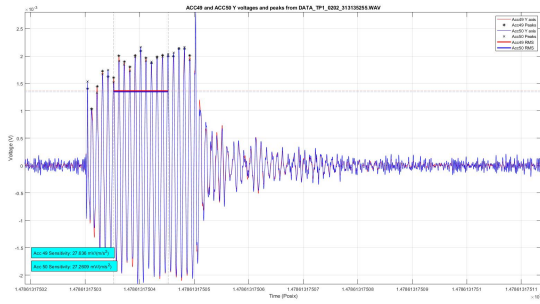


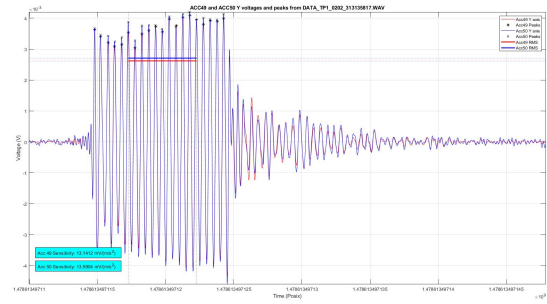
Figure B.27: Accelerometer waveforms for all axis at 4 kHz

## B.10 Y Axis Accelerometer voltage waveforms

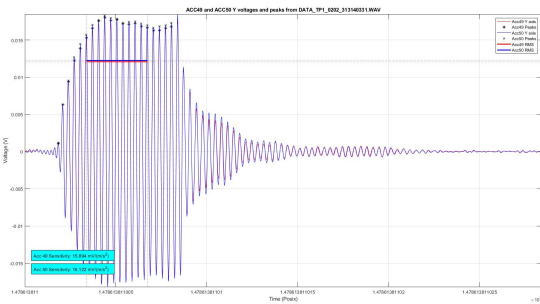
Following image show the waveforms for accelerometers at the 4 experiments, for ease comparison.



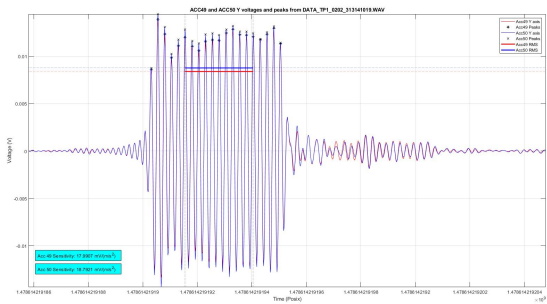
(a) 1 kHz



(b) 2 kHz



(c) 3 kHz



(d) 4 kHz

Figure B.28: Y axis accelerometers voltage comparison.

### B.11 3 Axis Accelerometers voltage waveforms for Y axis experiment

Following image show the waveforms for the 3 axis of each accelerometers at the 4 experiments, for ease comparison.

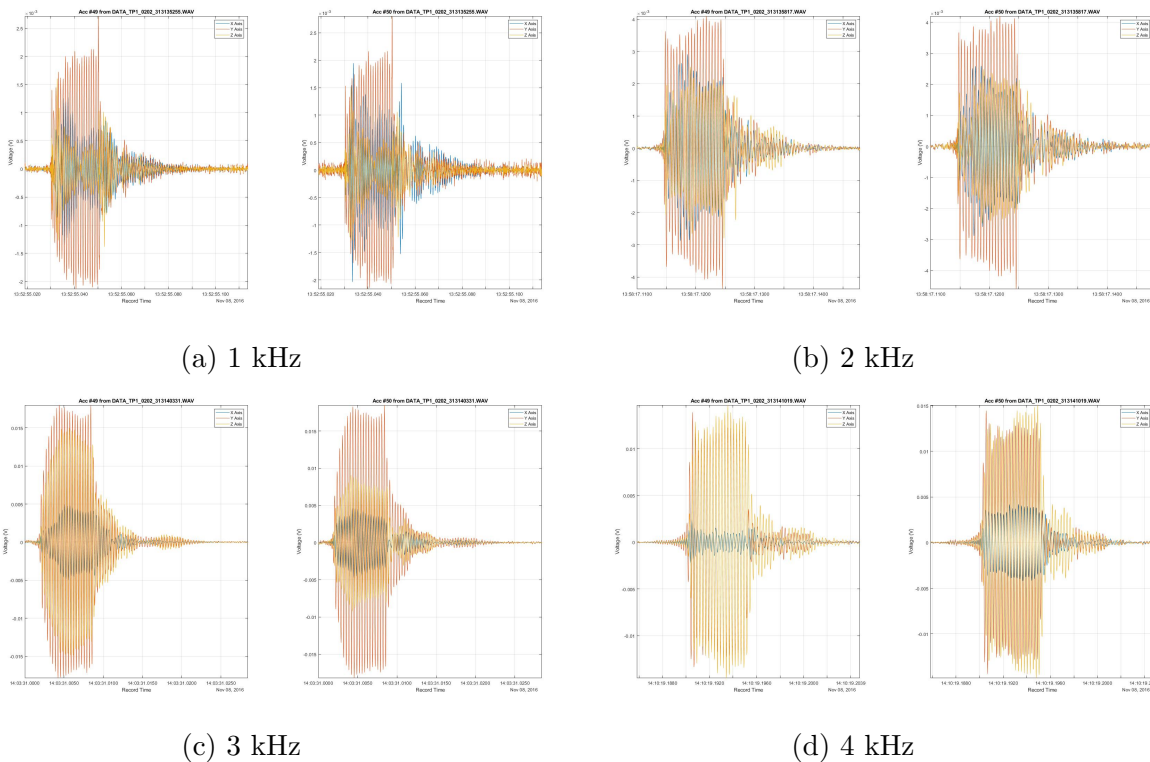
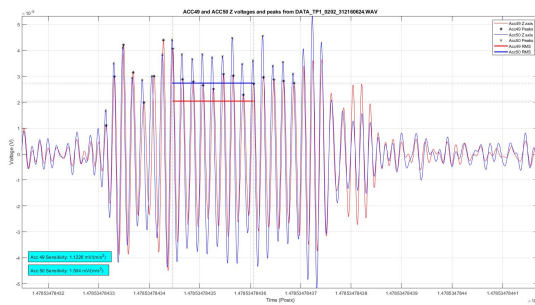


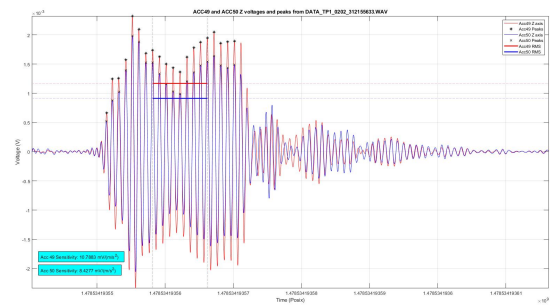
Figure B.29: Y axis accelerometers voltage waveforms for easy comparison. Each figure represent the captured waveforms from Y axis experiment, for the 4 used frequencies.

## B.12 Z Axis Accelerometer voltage waveforms

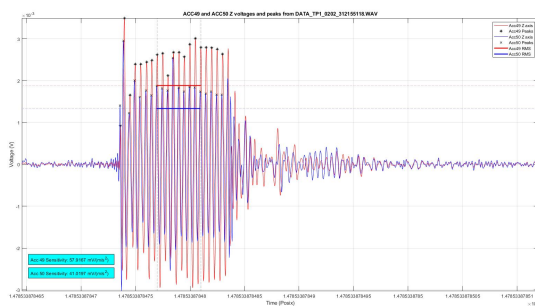
Following image show the waveforms for accelerometers at the 4 experiments, for ease comparison.



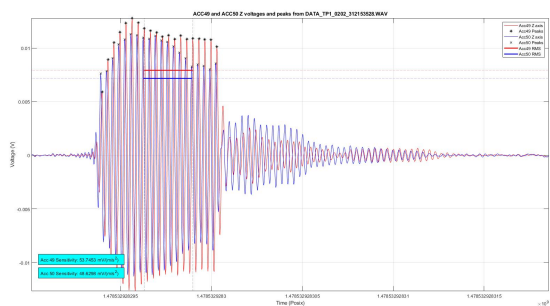
(a) 0.5 kHz



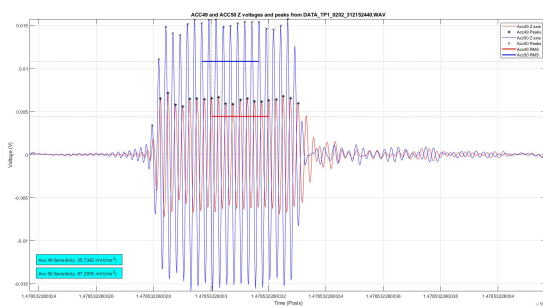
(b) 1 kHz



(c) 2 kHz



(d) 3 kHz



(e) 4 kHz

Figure B.30: Z axis accelerometers voltage comparison.

### B.13 3 Axis Accelerometers voltage waveforms for Z axis experiment

Following image show the waveforms for the 3 axis of each accelerometers at the 4 experiments, for ease comparison.

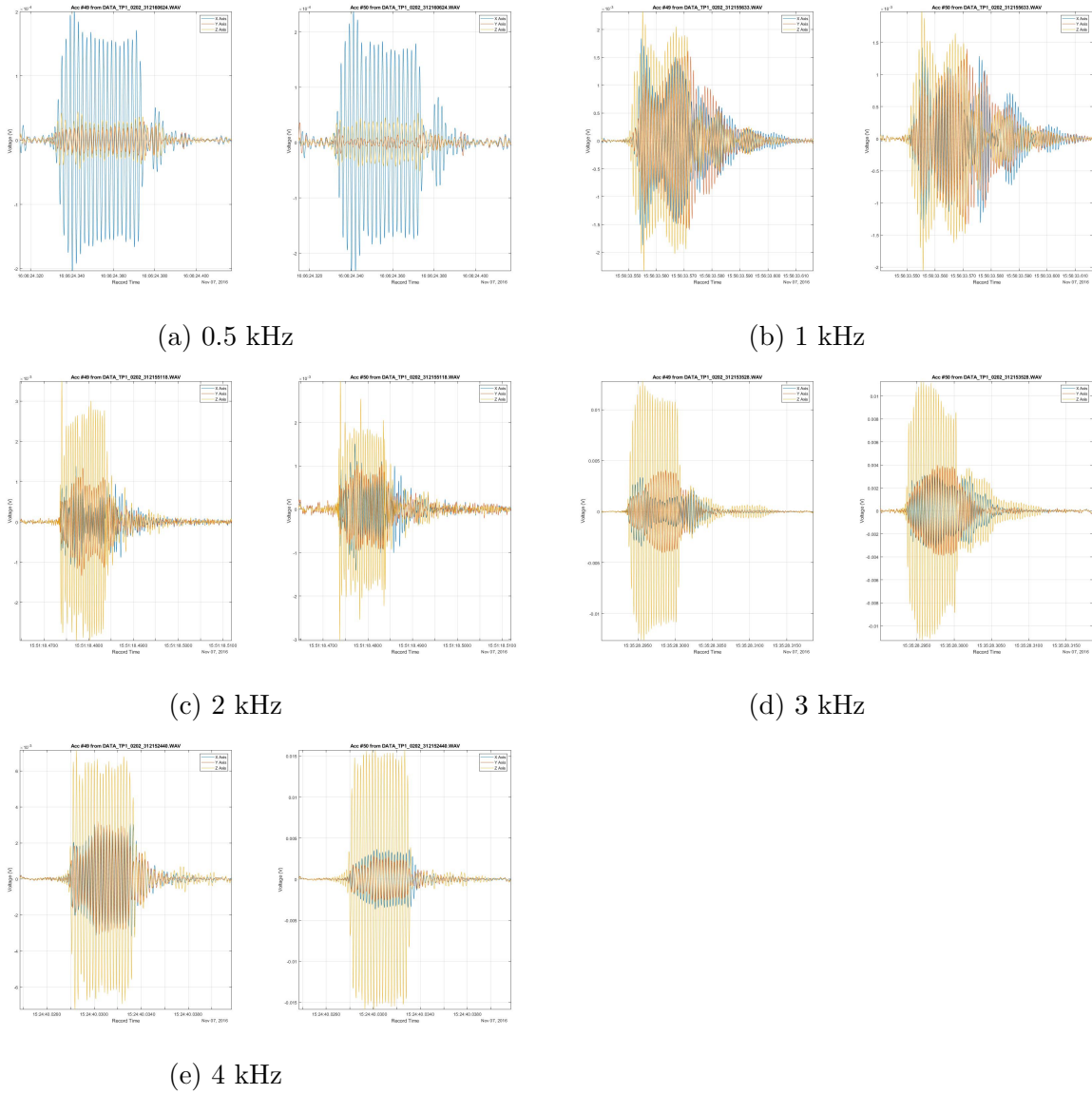


Figure B.31: Z axis accelerometers voltage waveforms for easy comparison. Each figure represent the captured waveforms from Z axis experiment, for the 4 used frequencies.

## C DAVS Directivity Waveforms

This chapter contains all the useful waveforms for the directivity experiments. The first subchapter contains the same graphs from the main text in a single figure to ease the comparison. The following subchapters contain the directivity plots for Y and Z axis on a single frequency, clockwise and counter clockwise rotations. The amplitude scale is between 0 and -20 dB, and the rotation scale starts at 0 degrees. For DAVS clockwise rotation, the graph follows the ascending angles (counter clockwise into plot, following 0°, 30°, 60°...). For counter clockwise rotation the graph is plotted inversely, in the clockwise direction (start at 0°, then -30°/330°, -60°/300°...). There's also a linear graph of the accelerometers normalized amplitude from the three axes, during the real time of capture. Overlaid in that graph is the rotation heading angle, allowing us to see the relative DAVS position and compare it with the response of accelerometers.

### C.1 Directivity Comparison

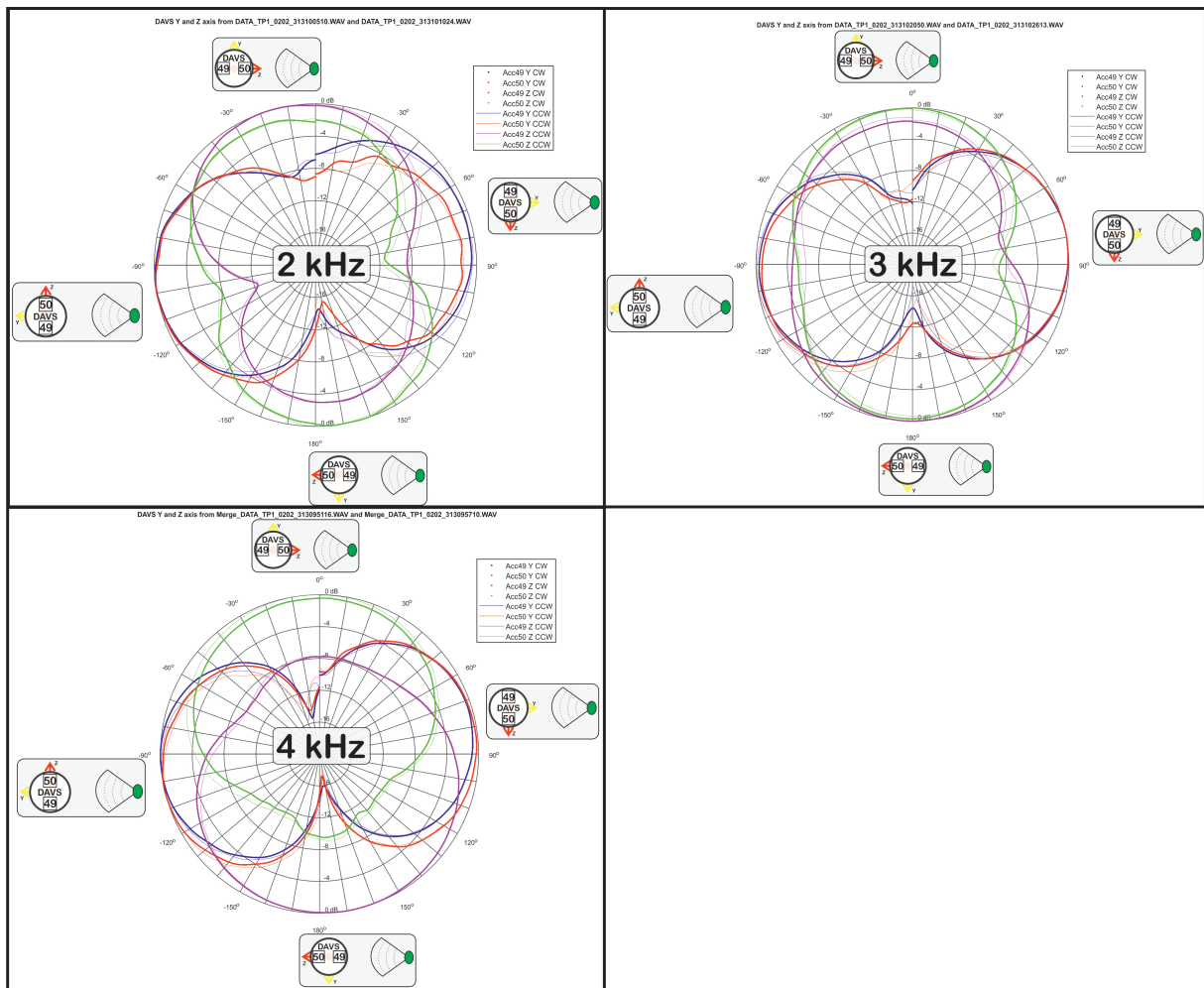


Figure C.1: Accelerometers directivity plot (for comparison)

### C.2 Setup 1 at 2 kHz

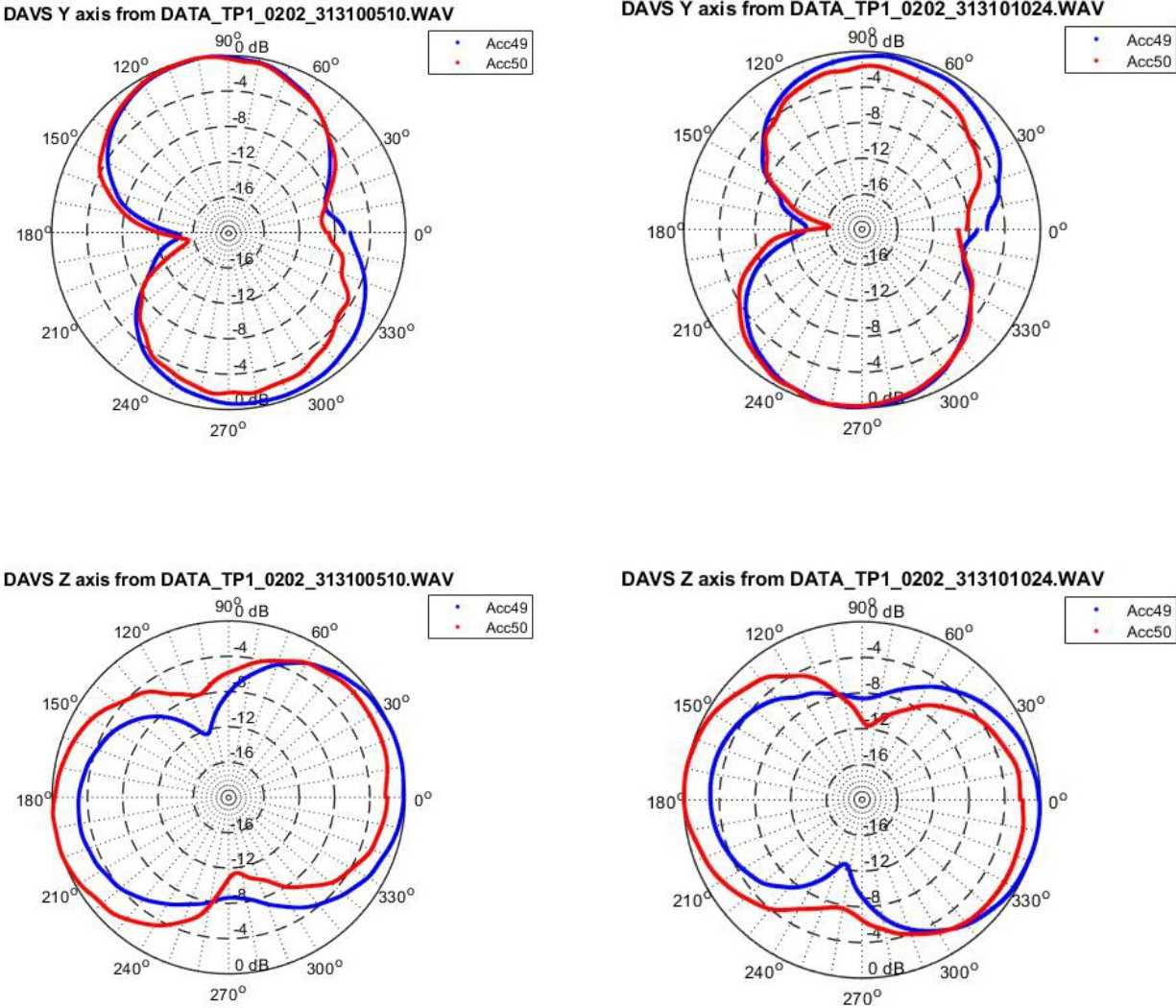


Figure C.2: Accelerometers response for setup 1 CW (left) and CCW (right) at 2 kHz

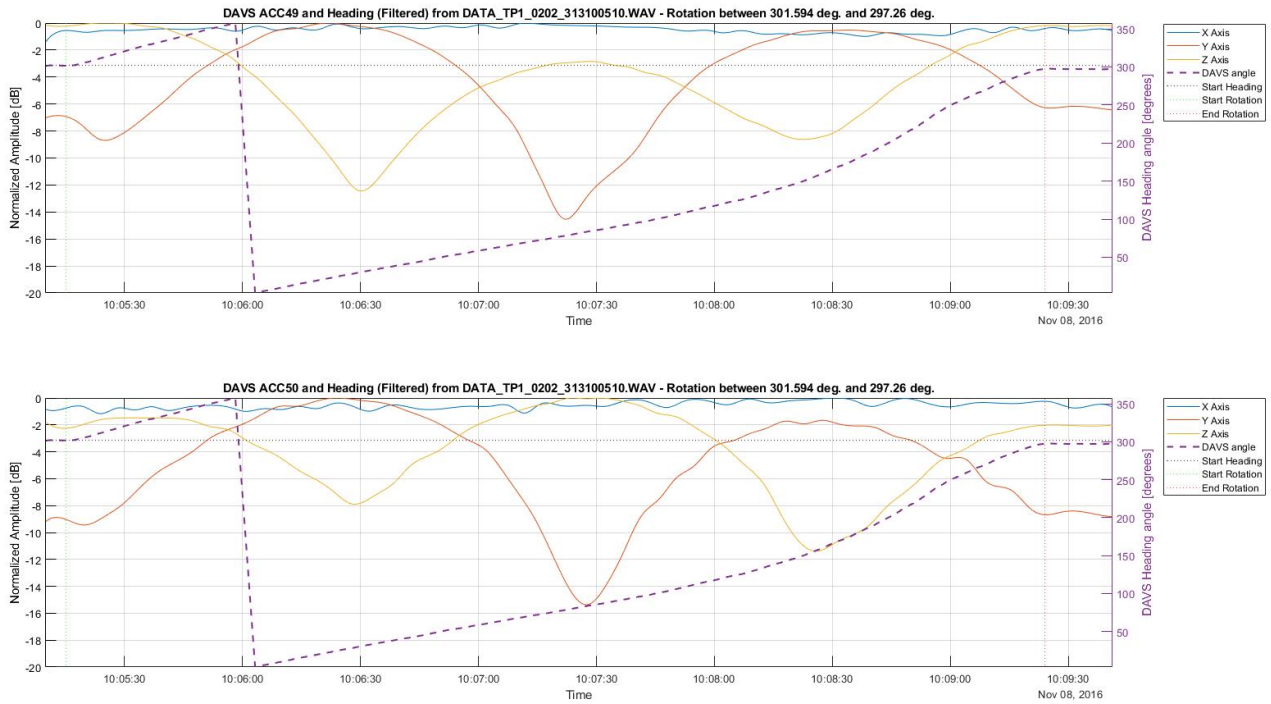


Figure C.3: Accelerometer waveforms and heading information for setup 1 CW at 2 kHz

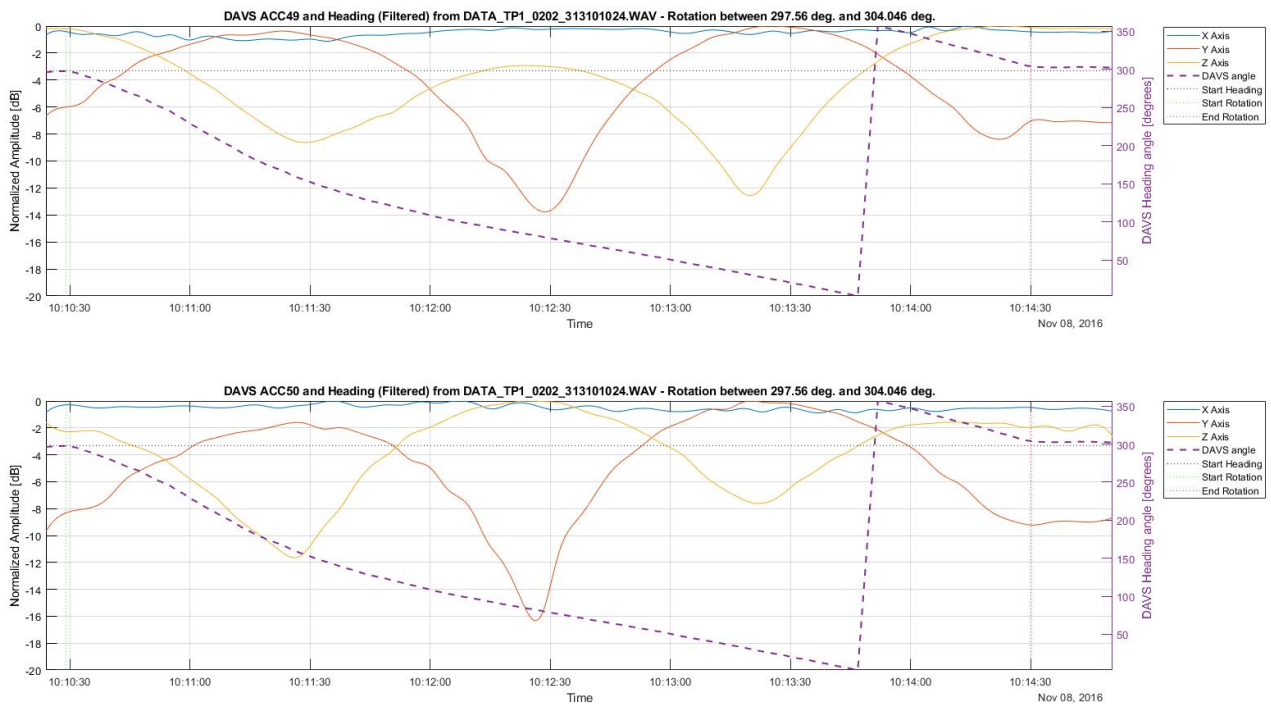


Figure C.4: Accelerometer waveforms and heading information for setup 1 CCW at 2 kHz

## C.3 Setup 1 at 3 kHz

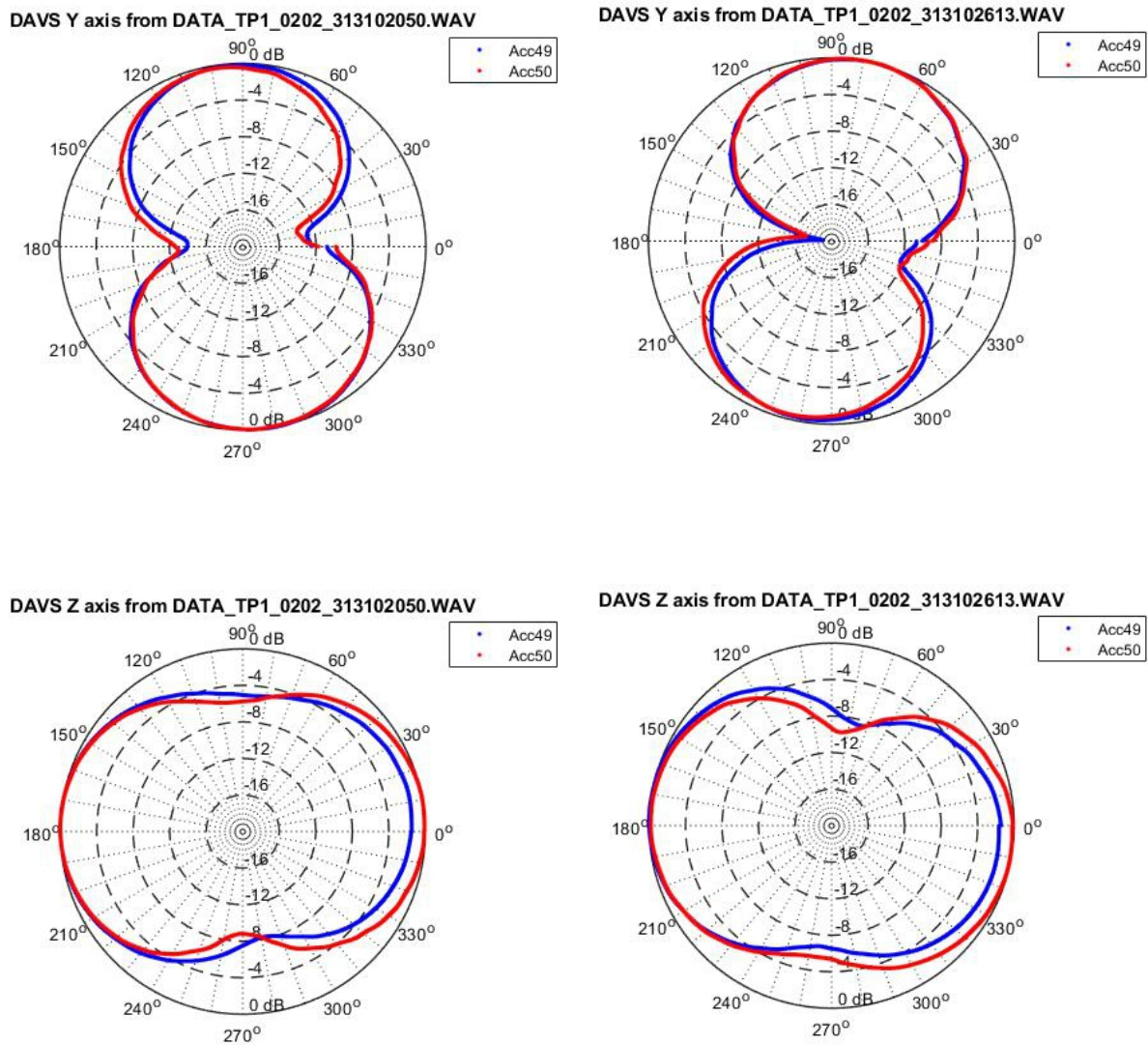


Figure C.5: Accelerometers response for setup 1 CW (left) and CCW (right) at 3 kHz

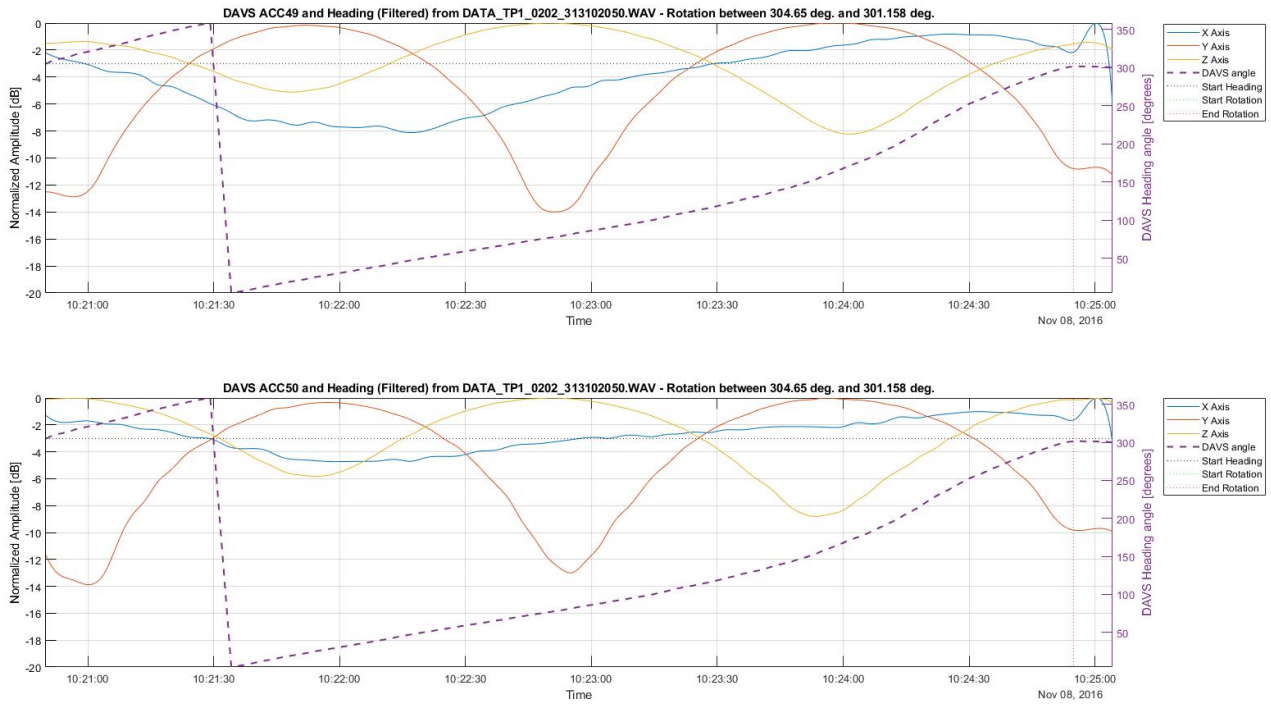


Figure C.6: Accelerometer waveforms and heading information for setup 1 CW at 3 kHz

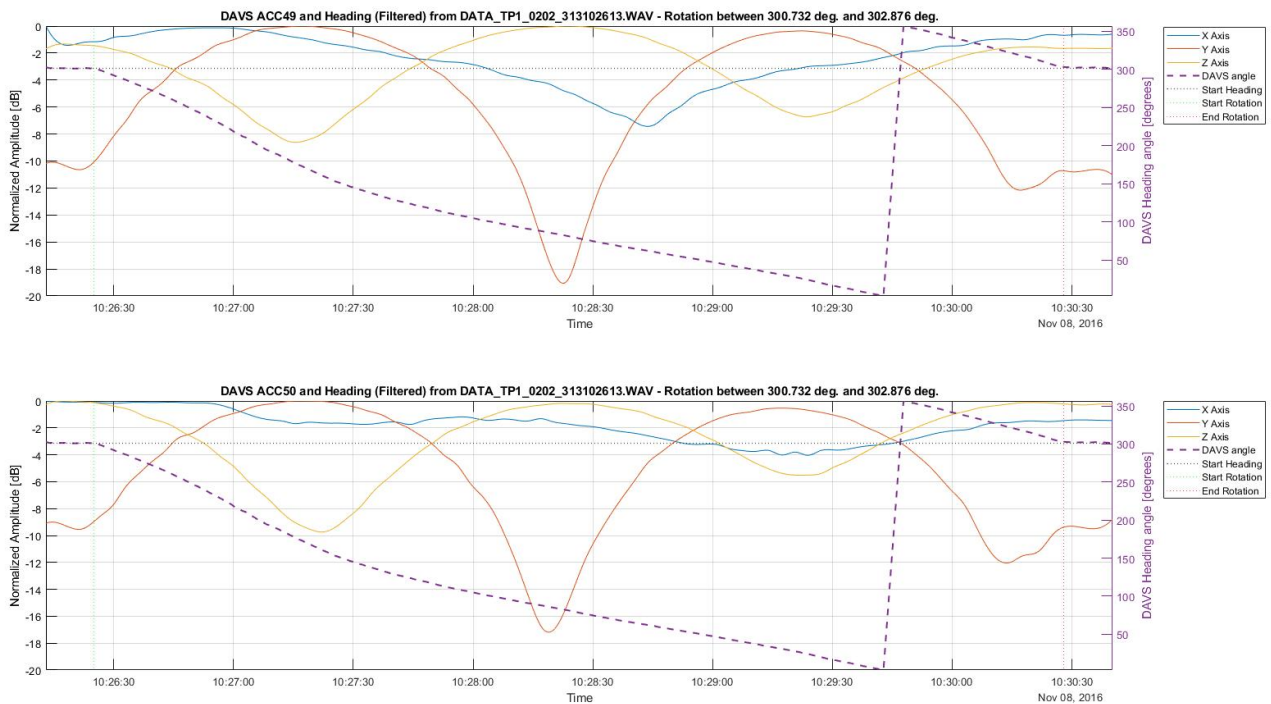


Figure C.7: Accelerometer waveforms and heading information for setup 1 CCW at 3 kHz

### C.4 Setup 1 at 4 kHz

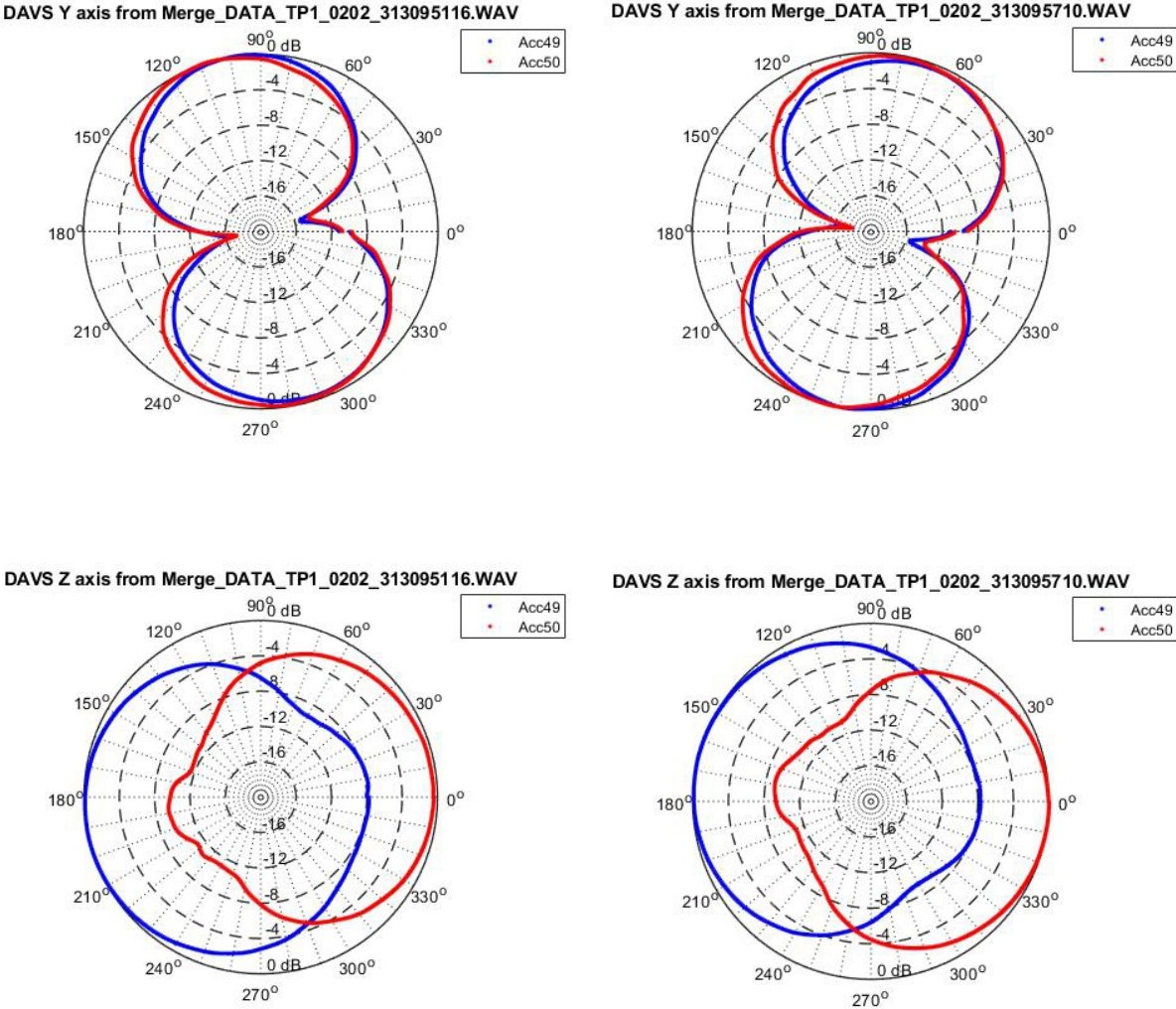


Figure C.8: Accelerometers response for setup 1 CW (left) and CCW (right) at 4 kHz

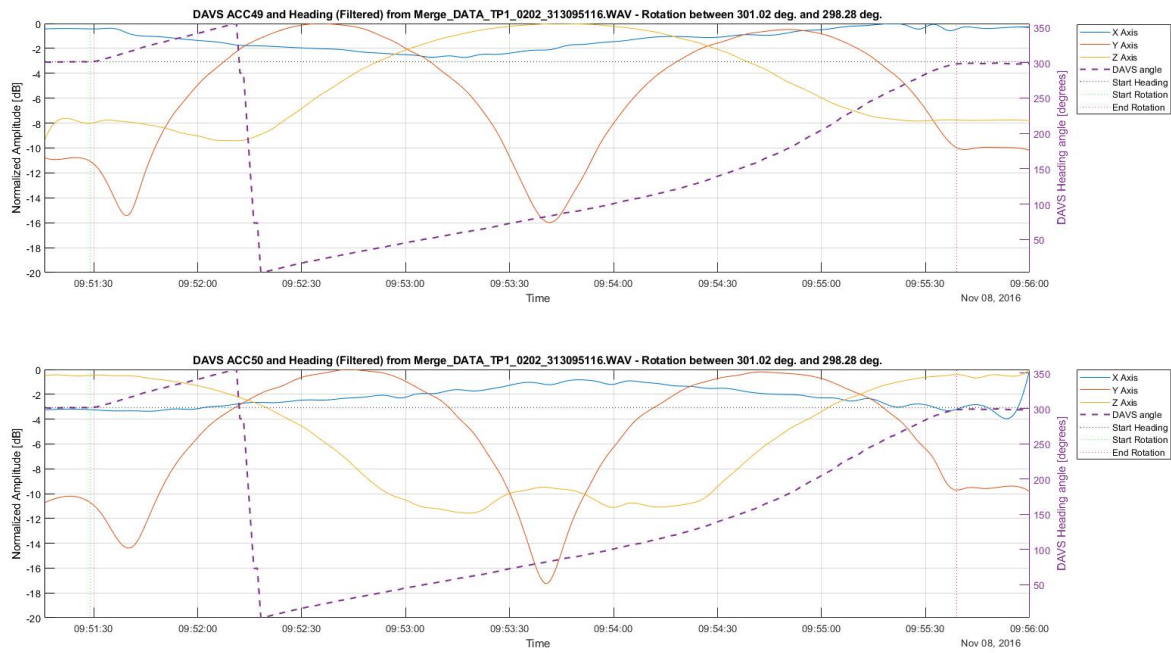


Figure C.9: Accelerometer waveforms and heading information for setup 1 CW at 4 kHz

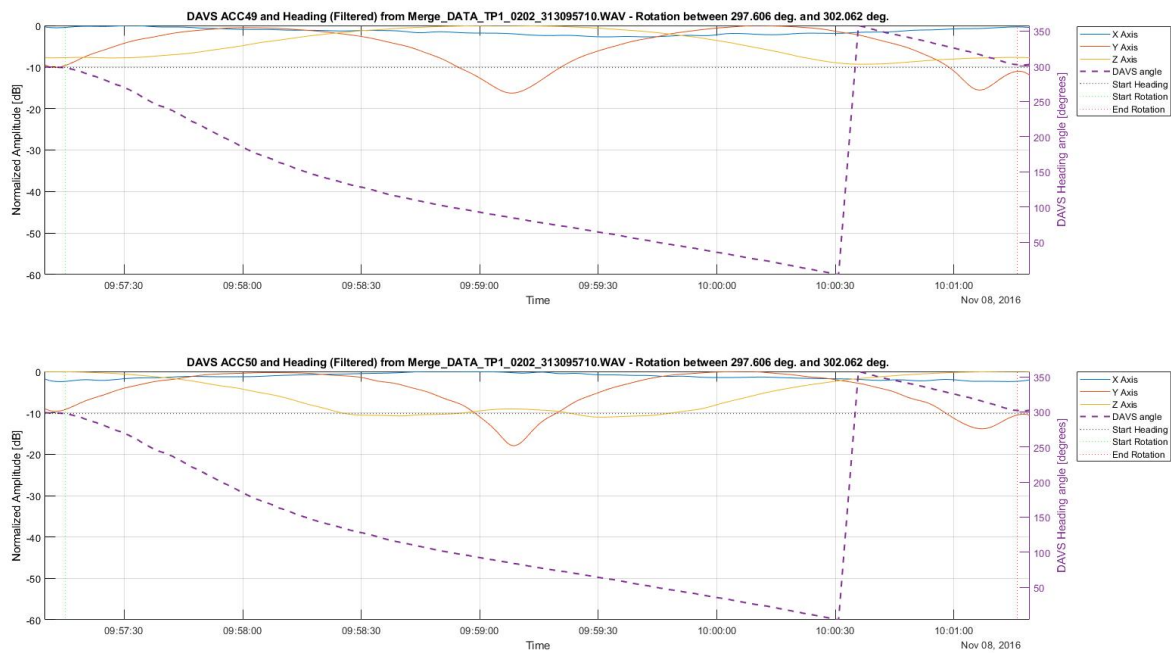


Figure C.10: Accelerometer waveforms and heading information for setup 1 CCW at 4 kHz

### C.5 Setup 2 and 3 at 2 kHz

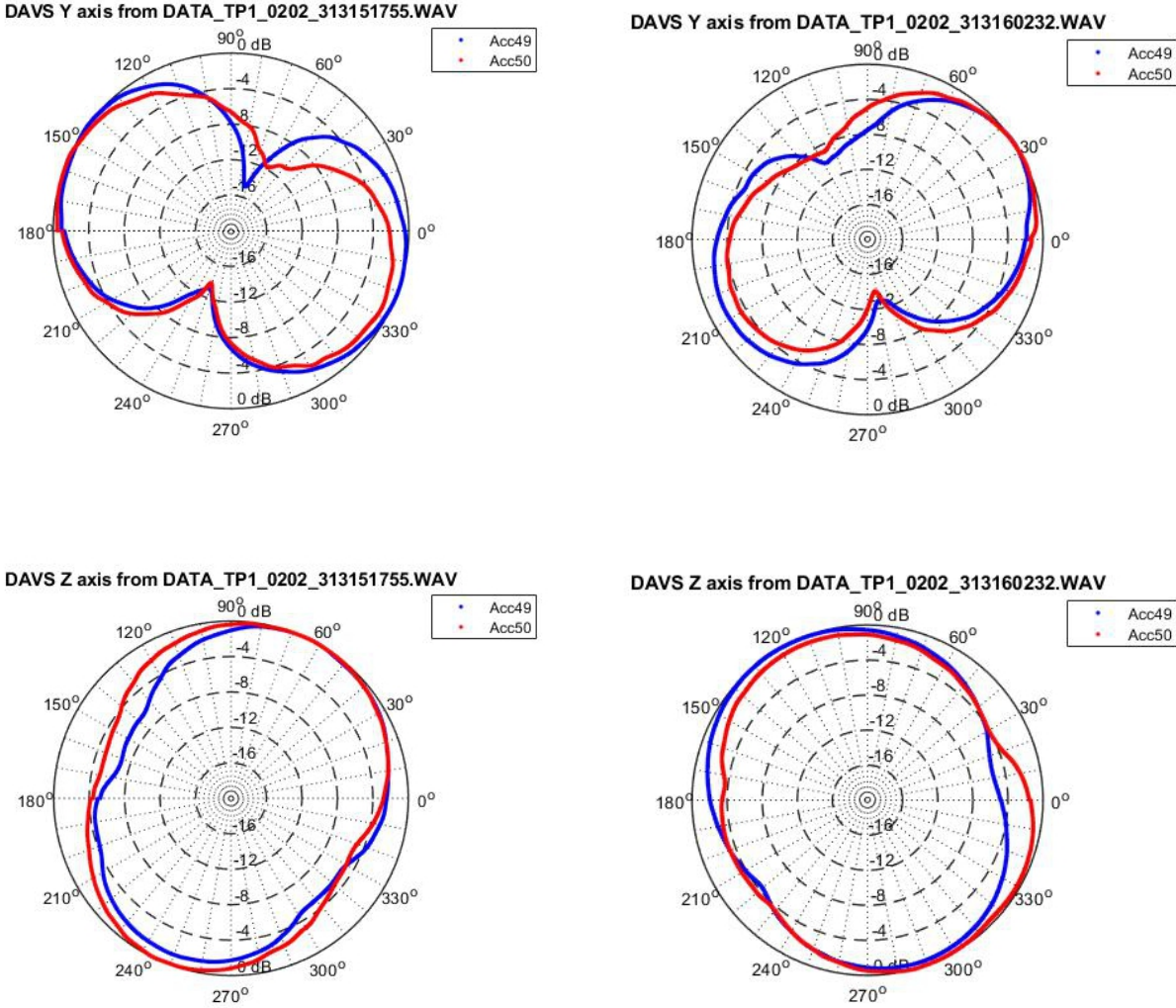


Figure C.11: Accelerometers response for setup 2 CW (left) and setup 3 CCW (right) at 2 kHz

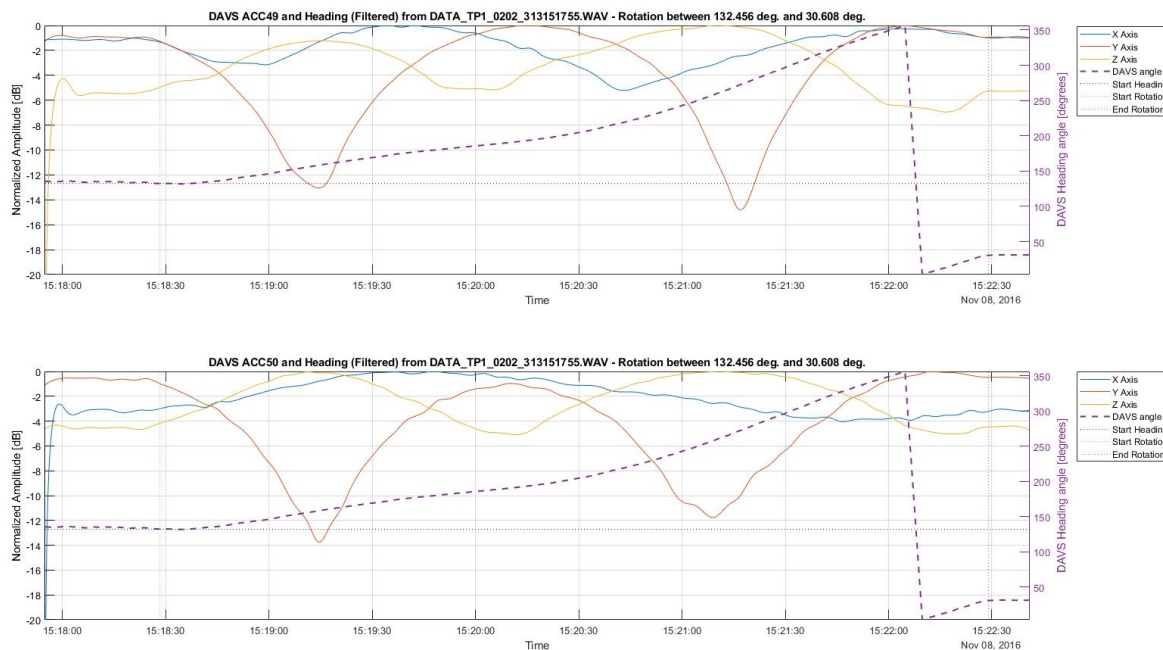


Figure C.12: Accelerometer waveforms and heading information for setup 2 CW at 2 kHz

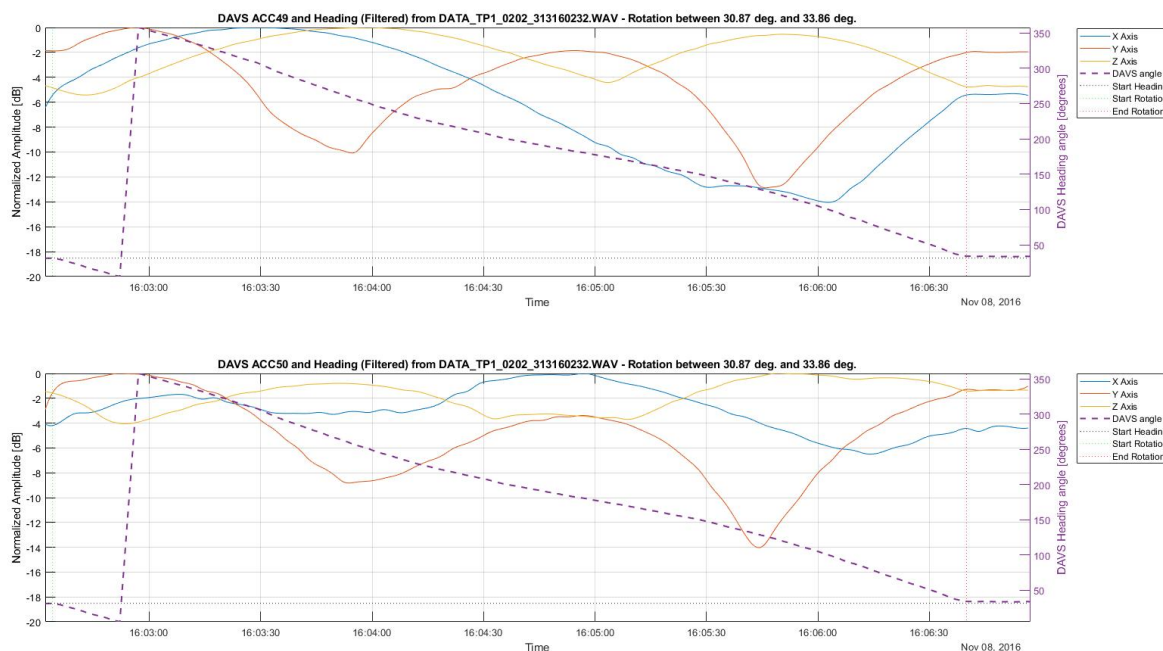


Figure C.13: Accelerometer waveforms and heading information for setup 3 CCW at 2 kHz